

12

AMMRC TR 82-20

AD

REQUIREMENTS FOR FLEXURE TESTING OF BRITTLE MATERIALS

AD A113937

FRANCIS I. BARATTA
MECHANICS OF MATERIALS DIVISION

April 1982

Approved for public release; distribution unlimited.

DTIC
ELECTE
APR 28 1982
S D

ARMY MATERIALS AND MECHANICS RESEARCH CENTER
Watertown, Massachusetts 02172

DTIC FILE COPY

82 04 28 009

DISCLAIMER NOTICE

**THIS DOCUMENT IS BEST QUALITY
PRACTICABLE. THE COPY FURNISHED
TO DTIC CONTAINED A SIGNIFICANT
NUMBER OF PAGES WHICH DO NOT
REPRODUCE LEGIBLY.**

The findings in this report are not to be construed as an official Department of the Army position, unless so designated by other authorized documents.

Mention of any trade names or manufacturers in this report shall not be construed as advertising nor as an official indorsement or approval of such products or companies by the United States Government.

DISPOSITION INSTRUCTIONS

Destroy this report when it is no longer needed.
Do not return it to the originator.

UNCLASSIFIED

SECURITY CLASSIFICATION OF THIS PAGE (When Data Entered)

REPORT DOCUMENTATION PAGE		READ INSTRUCTIONS BEFORE COMPLETING FORM
1. REPORT NUMBER AMMRC TR 82-20	2. GOVT ACCESSION NO. AD A113 987	3. RECIPIENT'S CATALOG NUMBER
4. TITLE (and Subtitle) REQUIREMENTS FOR FLEXURE TESTING OF BRITTLE MATERIALS		5. TYPE OF REPORT & PERIOD COVERED Final Report
7. AUTHOR(s) Francis I. Baratta		6. PERFORMING ORG. REPORT NUMBER
9. PERFORMING ORGANIZATION NAME AND ADDRESS Army Materials and Mechanics Research Center Watertown, Massachusetts 02172 DRXMR-SM		8. CONTRACT OR GRANT NUMBER(s)
11. CONTROLLING OFFICE NAME AND ADDRESS U. S. Army Materiel Development and Readiness Command, Alexandria, Virginia 22333		10. PROGRAM ELEMENT, PROJECT, TASK AREA & WORK UNIT NUMBERS AMCMS Code:728012.13
14. MONITORING AGENCY NAME & ADDRESS (if different from Controlling Office)		12. REPORT DATE April 1982
		13. NUMBER OF PAGES 46
		15. SECURITY CLASS (of this report) Unclassified
		15a. DECLASSIFICATION/DOWNGRADING SCHEDULE
16. DISTRIBUTION STATEMENT (of this Report) Approved for public release; distribution unlimited.		
17. DISTRIBUTION STATEMENT (of the abstract entered in Block 20, if different from Report)		
18. SUPPLEMENTARY NOTES		
19. KEY WORDS (Continue on reverse side if necessary and identify by block number) Mechanical tests Flexural strength Brittle materials		
20. ABSTRACT (Continue on reverse side if necessary and identify by block number) (SEE REVERSE SIDE)		

UNCLASSIFIED

SECURITY CLASSIFICATION OF THIS PAGE (When Data Entered)

UNCLASSIFIED

SECURITY CLASSIFICATION OF THIS PAGE(When Data Entered)

Block No. 20

ABSTRACT

Requirements for accurate bend-testing of four-point and three-point beams of rectangular cross-section are outlined. The so-called simple beam theory assumptions are examined to yield beam geometry ratios that will result in minimum error when utilizing elasticity theory. Factors that give rise to additional errors when determining bend strength are examined, such as: wedging stress, contact stress, load mislocation, beam twisting, friction at beam contact points, contact point tangency shift, and neglect of corner radii or chamfer in the stress determination. Also included are the appropriate Weibull strength relationships and an estimate of errors in the determination of the Weibull parameters based on sample size. Error tables, based on many of the previously mentioned factors, are presented.

Such data are utilized to rationally arrive at a 1/3-four-point and a three-point beam of a specific geometry ratio and dimension that will result in minimization of errors during flexure testing. Although such beams are recommended for a military standard, they are termed reference standard beams. Beams of other loading configurations and dimensions are considered acceptable if statistical correlation to one of the reference standards is determined, and if error spans are reported when presenting flexure test data.

Accession For	
NTIS GRA&I	<input checked="checked" type="checkbox"/>
DTIC TAB	<input type="checkbox"/>
Unannounced	<input type="checkbox"/>
Justification	
By	
Distribution/	
Availability Codes	
Dist	Avail and/or Special
A	



UNCLASSIFIED

SECURITY CLASSIFICATION OF THIS PAGE(When Data Entered)

CONTENTS

	Page
NOMENCLATURE.	111
INTRODUCTION.	1
OBJECTIVE	2
SIMPLE BEAM THEORY ASSUMPTIONS.	2
FOUR-POINT AND THREE-POINT LOADING.	7
EXTERNAL INFLUENCES	8
REFERENCE STANDARD BEAMS	
Geometry Ratios.	15
Beam Dimensions.	15
STRENGTH RELATIONSHIP AND SAMPLE SIZE	15
Volume-Sensitive Material.	16
Surface-Sensitive Material	17
Weibull Parameter Estimate and Sample Size	18
LOADING SPEED	20
DISCUSSION OF ERRORS.	21
Error Due to Load Mislocation.	21
Error Due to Beam Twisting	21
Error Due to Friction.	22
Error Due to Wedging Stress.	22
Error Due to Contact Point Tangency Shift.	22
Corner Radii	22
Error Span Summary	22
RECOMMENDATIONS AND CONCLUSIONS	23
TABULATIONS OF ERRORS IN CALCULATING FLEXURE STRESS	25
ACKNOWLEDGMENT.	30
REFERENCES.	30
Appendix A. Anticlastic Curvature.	31
Appendix B. Load Mislocation	32
Appendix C. Beam Twisting.	34
Appendix D. Wedging Stresses	37
Appendix E. Contact Point Tangency Shift	38
Appendix F. Error Due to Neglecting Change in Moment of Inertia Caused by Corner Radii or Chamfers	40

NOMENCLATURE

A_ℓ	Surface area of a rectangular beam stressed by four-point loading $A_\ell = 2\ell(b+d)$
A_L	Surface area of a rectangular beam stressed by three-point loading $A_L = 2L(b+d)$
ANS_4, ANS_3	Surface area of a nonstandard four-point and three-point loaded beam
ARS_4, ARS_3	Surface area of a reference standard four-point and three-point loaded beam
E	Young's modulus of the test material
E_C	Young's modulus in compression of the test material
E_T	Young's modulus in tension of the test material
G	Shear modulus of the beam material
I	Moment of inertia for a rectangular beam ($I = bd^3/12$)
$(I_{xx})_c$	Moment of inertia for a rectangular beam with 45° chamfered corners (see Appendix F)
$(I_{xx})_r$	Moment of inertia for a rectangular beam with rounded corners (see Appendix F)
L	Outer span length for a four-point and a three-point loaded beam
L_T	Total length of a beam
M	Weibull slope parameter associated with volume-sensitive material
M_b	General moment applied to beam
M_s	Weibull slope parameter associated with surface-sensitive material
M_x	Bending moment as a function of x (see Appendix D or E)
P	General applied force
P_1, P_2, P_3, P_4	Forces applied to a beam (see Figure 1)
R_{RS}	Risk of rupture - surface basis
R_{RV}	Risk of rupture - volume basis
T_b	Torque associated with beam twisting (see Figure 3 and/or Appendix C)
T_{be}	Estimated torque when bottoming within the load fixture occurs (see Appendix C)
V_ℓ	Volume of a four-point loaded beam ($V_\ell = \ell bd$) in the risk of rupture equation.
V_L	Volume of a three-point loaded beam ($V_L = Lbd$) in the risk of rupture equation
V_{NS_4}, V_{RS_4}	Volume of the centrally loaded section of the nonstandard and reference standard four-point loaded beam
V_{NS_3}, V_{RS_3}	Volume of the nonstandard and reference standard three-point loaded beam
a	Half the distance between the inner span and outer span for a four-point loaded beam, i.e., $(L-\ell)/2$ or $a=L/2$ for a three-point loaded beam (note $a_1 = a_2 = a$)

a_1 and a_2	A beam dimension (see Figures 1 and 2)
b	Beam width (see Figure 1 or 5)
c	Chamfer of a corner of a beam with 45° chamfers (see Figure 5)
d	Beam depth (see Figure 1 or 5)
e	Load eccentricity equal to $(a_1 - a)$
e/L	Load eccentricity ratio equal to $(a_1 - a)/L$
e_c	Shift of neutral axis in an initially curved beam
h_1, h_2	Horizontal shift of contact and load points due to beam bending (see Figure 4)
k_1, k_2	A numerical factor dependent upon b/d (see Appendix C)
l	Inner span length of a four-point loaded beam (see Figure 1)
l'	Either equal to "a" or $L/2$ for four-point or three-point beam systems
n	Numerical factor (see Equation 14b)
p_{max}	Maximum contact pressure at the load application point
r	Radius of the corners of the beam (see Figure 5)
s	Speed of loading
t	Time of loading
x_1, x_2, x_3	Variable beam distances (see Figure 1c)
x'	Variable distance (failure site location) on either side of the load contact point (see Appendix D)
x, y	Coordinate axes (see Figure 1)
α_b, α_c	Beam curvature parameters (see Equations 3a and 4a)
β	Anticlastic curvature factor (see Appendix A)
β_T	A numerical factor associated with the tensile stress caused by load contact (see Appendix D)
γ	$\gamma = \sqrt[4]{3(1-\nu^2)/d^2\rho^2}$ (see Appendix A)
$\epsilon_x, \epsilon_y, \epsilon_z$	Strain in the x, y, and z directions
$\dot{\epsilon}$	Strain rate
$\bar{\epsilon}$	Percent error, usually defined as $[(\sigma_b - \sigma_x)/\sigma_x]100$
θ	Angle of a plane inclined to x-axis
θ^*	Angle of a plane inclined to the x-axis at which the principal stress is maximum
λ	Surface area parameter (b/d)
$\lambda_{NS_4}, \lambda_{NS_3}$	Surface area parameter of a nonstandard four-point and three-point loaded beam
$\lambda_{RS_4}, \lambda_{RS_3}$	Surface area parameter of a reference standard four-point and three-point loaded beam
μ	Coefficient of friction

ν	Poisson's ratio
ρ	Radius of a curvature of a beam due to bending
ρ_1	Contact radius of a support point (see Figure 4)
ρ_2	Contact radius of a load point (see Figure 4)
ρ_c	Initial radius of the curvature of a beam
σ_b	Bending stress in a beam as defined by simple beam theory or mean fracture stress
$\sigma_{bns_{4,3}}$	Average bending stress of a nonstandard four-point and three-point loaded beam
$\sigma_{bRs_{4,3}}$	Average bending stress of a reference standard four-point and three-point loaded beam
σ_n	Normal stress (see Appendix C)
$\sigma_{n_{max}}$	Maximum principal stress (see Appendix C)
σ_o	Scale parameter or characteristic value associated with a Weibull analysis
σ_x	Stress in the x direction (along the beam length)
σ_z	Stress in the z direction (along the beam width)
τ	Shear stress due to torsion (see Appendix C)
ϕ_s	Angle of twist along the specimen length (see Figure 3 and Appendix C)
ϕ_F	Angle of twist between a pair of load and contact points relative to ϕ_s (see Appendix C)

INTRODUCTION

There has been an increase in interest and activity in recent years in both the research and development of ceramic materials and their practical application to engineering structures. Much of the impetus is due to the Defense Advanced Research Projects Agency (DARPA) program¹ where the objective is to develop ceramic turbine engines for vehicular use and electric power generation. It was recognized* during the course of this program that technical progress would be improved by having available unified standard testing methods so that the interchange of test data between involved organizations would have the same reference base. This requirement is vital because ceramic materials need particular kinds of mechanical tests suitable to their brittle nature so that valid test data will result.

Action was initiated to determine what kind of standards, if indeed any, were available for mechanical testing of brittle materials.† It was determined from this study that "of some 80-odd existing ceramic standards reviewed (c.f. NBS SP 329, and Index of U.S. Voluntary Engineering Standards and DoD Index of Specifications and Standards), only one was found suitable for testing structural ceramics. An in-house review and survey of cognizant government and nongovernment activities confirmed both the lack of test method standards, and the real need for such standards."

As a result of the above exercise, a tentative unapproved set of standards‡ was prepared by the Army Materials and Mechanics Research Center (AMMRC) and distributed to interested and involved organizations. This set of unofficial standards, which included such test methods as flexure, tension, creep, stress rupture, fatigue, and spin testing, was discussed at several meetings of government and industry representatives. A number of worthwhile suggestions evolved. However, it was apparent that these tentative standards could be improved, and such comments were invited.

These unofficial standards have remained unchanged and unapproved. Recently, however, interest was revived at AMMRC in finalizing standard tests for brittle materials. It was viewed that the original tentative standards, dated 2 April 1973, represented the ideal goal but were far too inclusive to realistically establish testing requirements which would provide valid results at this time. It had also been decided that each subject should be separately treated as sufficient test methodology knowledge evolved. Since flexure testing to determine bend strength met this criterion, it was decided to standardize such a test. Other specific recommendations regarding flexure testing resulting from the AMMRC committee were proposed and are as follows:

The standard at the present time would consider only beam testing methodology.

The test would have to conform within the requirements of simple beam theory, thus the test would be restricted to a temperature environment of 70°F or less.

*The Ford Motor Company, in a letter dated 31 April 1972, cited the problem of nonexistent standards for testing structural ceramic materials and appealed to AMMRC to initiate action to develop appropriate standards.

†Trip to Ford Motor Company, Dearborn, Michigan, on 9 May 1973, by H. F. Campbell, S. Acquaviva, and L. G. MacDonald, dated 15 May 1973.

‡Army Materials and Mechanics Research Center, "Military Standards - Test Methods for Structural Standards," 2 April 1973.

1. VAN REUTH, E. C. *The Advanced Research Projects Agency's Gas Turbine Program*. Proc. of the Second Army Materials Technology Conference - Ceramics for High Performance Applications, J. J. Burke, A. E. Gorum, and R. N. Katz, ed., Brook Hill Publishing Company, Chestnut Hill, Massachusetts, 1974.

Although two beam testing systems are to be used, i.e., size, dimensions, loadings, etc., and called *reference standards*, other systems will be acceptable as long as strength relationships are determined and an estimate of the errors are reported along with the test data results.

The author, who had presented a critique* of the tentative standard, was charged with the task of providing backup material in the form of a formal report. This work is a result of that request.

OBJECTIVE

The objective of this report is to recommend beam test systems such that accurate fracture strength utilizing simple beam theory will result. Such recommendations will be used as the basis of a military standard for flexure testing of brittle materials within the elastic regime.

SIMPLE BEAM THEORY ASSUMPTIONS

The rectangular beam configuration is attractive as a strength-test vehicle because of its simple shape and apparent ease of load application, as well as analysis and reduction of data. Rods of circular cross section are also used in beam tests, but usually for specialized testing. Because a beam of circular cross section is not as frequently used as the rectangular beam, the circular cross section is not considered a reference standard candidate; therefore only the rectangular cross section is examined in the discussions to follow.

A critical review of simple beam theory assumptions will yield ranges of geometry ratios by which the theory can be validly applied. These assumptions are listed below, as well as their associated inferences in terms of an error analysis:

1. Transverse planes perpendicular to the longitudinal axis of the beam remain plane after the beam is bent.
2. The modulus of elasticity in tension is equal to the modulus of elasticity in compression. Also, the beam material is isotropic and homogeneous.
3. The maximum deflection must be small compared to the beam depth.
4. The beam must deflect normally under elastic bending stresses but not through any local collapse or twisting.

Each of the above assumptions is examined in detail, where possible, so that the required rectangular beam geometry ratios can be determined as a function of the associated errors.

Assumptions 1 and 2 together imply that stress and strain are proportional to the distance from the neutral axis, and the stress does not exceed the proportional limit of the material. These assumptions disregard the effect of any shearing resistance and make impossible the use of the flexure formula for curved beams of large curvature.

*Memorandum - Review of "Military Standard Test Method for Structural Ceramics," by F. I. Baratta, AMMRC, December 1973, revised February 1974.

Assumption 1 and the above implication infer that there is a linear relationship of stress between the fibers of the beam. Timoshenko and Goodier² give the more exact distribution of stress as the function of the distance from the neutral axis for a simply supported beam loaded by distributed pressure. Although the candidate beams to be considered here will be four-point and three-point loaded beams, these different loading conditions should not yield markedly different results from those taken from the above reference.* From Reference 2 an estimate of the error incurred when assuming a linear stress distribution can be obtained from the following equation:

$$\sigma_x = \sigma_b \left[1 + \left(4/15 \right) \left(\frac{1}{L/d} \right)^2 \right]. \quad (1)$$

The above equation is approximately applicable for both four-point and three-point loading. The beam geometries and loading configurations considered are shown in Figures 1a and 2a. The error resulting from assuming a linear stress distribution when in fact nonlinearity exists is given in Table 1. (Tables begin on page 25.)

Regarding the assumption that the modulus of elasticity in tension is equal to that in compression, $E_T = E_C$, Chamlis³ has derived in closed form the solution for the tensile bending stress when $E_T \neq E_C$. After some manipulation of appropriate formulas in Reference 3, the tensile stress due to bending is given by:

$$\sigma_x = (\sigma_b/2) [1 + (E_T/E_C)^{1/2}], \quad (2)$$

for both the four point and the three-point loaded beams. The resulting percent error is given in Table 2.

Although the errors associated with neglecting to account for anisotropy and nonhomogeneity of the test material are not considered here, they are briefly mentioned in the following paragraphs so that the reader will be aware of such possibilities.

If the beam is anisotropic, the bending stress formula is exactly the same as the elementary theory except that the application of a bending moment produces a twisting moment, and vice versa. According to Lekhnitskii,⁴ determining the accompanying shear stress produced by bending a rod of rectangular cross section, having only one plane of elastic symmetry normal to the axis, is very complicated. (Composite and crystal structures are excluded here as test materials.) If the degree of anisotropy for ceramic material is slight, it may be permissible to assume that the error when ignoring this effect on the fracture stress will also be small.

Nonhomogeneity of the test material infers variation of the elastic modulus. It has been observed† that in plates of hot-pressed silicon nitride, the modulus of elasticity at the surface is several percent different than that of the center. This

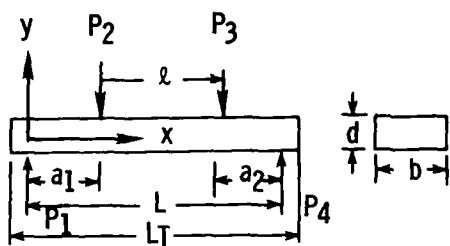
*Recent finite element computer results by H. Faou and R. J. H. Bollard of the University of Washington indeed show this to be true. See Flexure Test Method T10, Proceedings of the Sixth Army Materials Technology Conference, "Ceramics for High Performance Applications - III - Reliability," held at Orcas Island, Washington, July 1979.

†Private discussion with E. M. Lenoe, AMMRC.

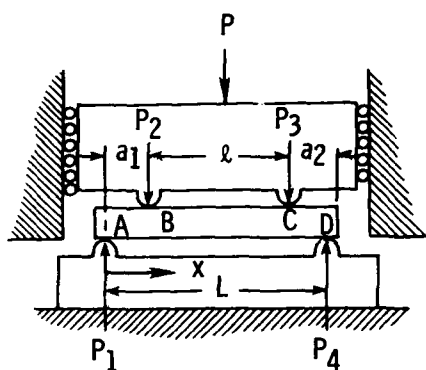
2. TIMOSHENKO, S., and GOODIER, J. N. *Theory of Elasticity*. 2nd Ed., McGraw-Hill Book Co., Inc., New York, 1951.

3. CHAMLIS, C. C. *Analysis of Three-Point-Bend Test for Materials with Unequal Tension and Compressive Properties*. NASA TN D7572, March 1974.

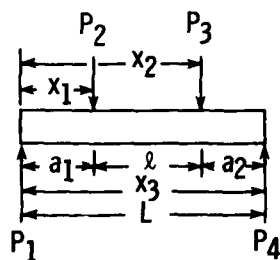
4. LEKHNITSKII, S. G. *Theory of Elasticity of an Anisotropic Elastic Body*. Holden-Day Series in Mathematical Physics, J. L. Brandstatter, ed., 1963, p. 204.



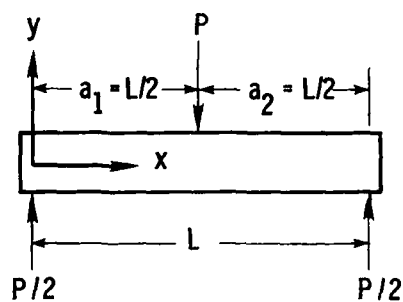
(a) Idealized Loading $a_1 = a_2 = a$



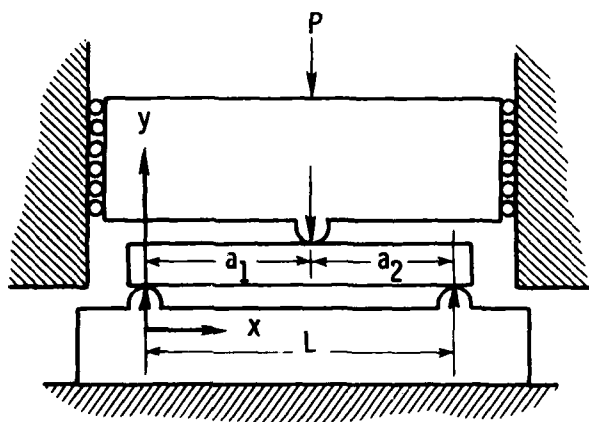
(b) Nonpivoting Rigid Loading Head
 $a_1 \neq a_2$



(c) Loading when $x_1 \neq x_3 - x_2$



(a) Idealized Loading



(b) Nonpivoting Rigid Loading Head; $a_1 \neq a_2 \neq L/2$

Figure 1. Four-point loading.

Figure 2. Three-point loading.

is also an area in which further analysis will be required to assess the error applicable to four-point and three-point loaded beams when the modulus of elasticity varies through the beam thickness.

If a rectangular beam has initial curvature ρ_c , the error can be determined from an analysis provided by Timoshenko.⁵ The general bending stress σ_x in a curved beam due to a pure moment is given by the following:

$$\sigma_x = \alpha_c (M_b / b d \rho_c) \quad (3)$$

where

$$\alpha_c = \frac{(d/2\rho_c) - (e_c/\rho_c)}{(e_c/\rho_c)[1 - (d/2\rho_c)]} \quad (3a)$$

$$e_c/\rho_c = [(d/\rho_c)^2/12][1 + (d/\rho_c)^2/15]. \quad (3b)$$

Since the bending stress, according to simple beam theory, is $\sigma_b = 6M_b/bd^2$, and putting σ_b in the same terms as (3) above, we have:

$$\sigma_b = \alpha_b (M_b / b d \rho_c), \quad (4)$$

where

$$\alpha_b = 6(\rho_c/d). \quad (4a)$$

The percent error $\bar{\epsilon}$ for a bent beam of rectangular cross section and of beam-to-depth initial curvature ρ_c/d resulting in a neutral axis shift of e_c/ρ_c is:

$$\bar{\epsilon} = 100[(\alpha_b - \alpha_c)/\alpha_c]. \quad (5)$$

The resulting error for a beam of rectangular cross section bent by a pure moment as obtained from (5) is given in Table 3 as a function of initial curvature. It is assumed that an analogous analysis applied to a three-point loaded beam would produce similar results.

The validity of the inference that the strain is proportional to the distance from the neutral axis is dependent upon the ratio of the beam width to its depth. Anticlastic curvature of rectangular beams or plates with intermediate ratios of b/d can lead to erroneous results using simple beam theory; see Timoshenko.⁶ Of course, if the beam can be considered infinite in width, like a plate, the correction of the bending stress is simply $1/(1 - \nu^2)$. The question arises as to what ratios of b/d are appropriate for the application of simple beam theory. Ashwell⁷ examined in detail the anticlastic curvature of rectangular beams and plates and provided the answer to this question. The pertinent formulas taken from Reference 7 are given in Appendix A. These equations were applied to ceramic materials with Poisson's ratio ν equal to 0.25 and the ratio of Young's modulus to fracture stress E/σ_b of 1×10^3 to determine the percent error* using simple beam theory as a function of b/d which is shown in Table 4.

*Ashwell considered a beam bent by a constant moment analogous to the four-point beam loading case, which should represent a conservative bound on b/d for the three-point beam, as well.

5. TIMOSHENKO, S. *Strength of Materials*. Parts I and II, D. Van Nostrand Co., Inc., New Jersey, 1976.

6. TIMOSHENKO, S. *Letter to the Editor*. *Mechanical Engineering*, v. 45, no. 4, April 1923, p. 259-260.

7. ASHWELL, D. G. *The Anticlastic Curvature of Rectangular Beams and Plates*. *J. Roy. Aero. Soc.*, v. 54, 1950, p. 708-715.

If the maximum deflection is not small compared to the beam depth, linear beam theory cannot be employed without an error. West⁸ examined large deflections of three-point loaded beams, and from such results a definitive ratio of beam length to depth can be determined for valid application of simple beam formulas. Since for most brittle materials values of E/σ_b range from approximately 0.5×10^3 to 1×10^3 , the former value was used to compute the percent error because it would yield the largest error. Although the analysis was applied to a three-point loaded beam, the method was extended to determine errors for four-point loaded beams as well. The results of the calculations using the mentioned analysis⁸ are presented in Table 5, which gives errors for a 1/3-four-point, a 1/4-four-point, and a three-point loaded beam as a function of L/d .

It is implicit in the assumptions given in Reference 8 that the loads and moments are applied to the beam in an ideal manner with no friction occurring between the load application points and the beam. Ritter and Wilson⁹ have determined a beam length-to-depth limit based on the minimization of friction effects when large deflections occur. The friction effect considered is that which gives rise to a moment caused by the slope at the load application point. Not considered in the analysis⁹ are the effects of friction due to a moment acting out of the neutral plane of the beam, lateral contraction or extension, and changes in moment arms due to contact point tangency shift. These factors will be discussed later.

Returning to the results of Reference 9, an inequality for the four-point-loaded beam which provides a limit is given in the following:

$$(L/d - a/d)/(E/\sigma_b) \leq 0.3 \quad (6)$$

to insure negligible nonlinear deflections and friction effects. The value of 0.3 was obtained from limiting the slope to less than 15° between the beam in the loaded and unloaded positions at the outermost support point. If the minimum value of E/σ_b is chosen to be 0.5×10^3 , then we determine that for a four-point loaded beam (6) becomes:

$$L/d - a/d \leq 150. \quad (7)$$

It is noted from Table 5 that neglecting beam deflections resulted in greater error in calculation of bending stress for the four-point loaded beam than for the three-point loaded beam. For conservatism, therefore, it will be assumed that (7) is applicable to the three-point loaded beam as well, with $a/d = 0$. Thus (7) becomes

$$L/d \leq 150. \quad (8)$$

It appears that these limits are compatible with those values given in Table 5 such that reasonable L/d ratios can be chosen that will result in small errors when minimizing deflection.

One of the last requirements, no buckling of the beam, is easily fulfilled for ceramic materials with beam dimensions of practical test configurations. The reader can readily verify this statement by referring to Timoshenko and Gere.¹⁰

Accuracy, which is inferred in the above restrictions, is also dependent upon the manner of load application, beam geometry, loading fixtures, and surface preparation. Although specimen size will not affect accuracy except for extremely small geometries,

8. WEST, D. C. *Flexure Testing of Plastics*. Exp. Mech., v. 21, no. 2, July 1964.

9. RITTER, J. E., and WILSON, W. R. D. *Friction Effects in Four-Point Bending*. ASLE Transactions, v. 18, no.2, p. 130-134, presented at the 29th annual meeting, April 28-May 2, 1974.

10. TIMOSHENKO, S., and GERE, J. M. *Theory of Elastic Stability*. McGraw-Hill Book Co., Inc., New York, 1961.

it will alter the magnitude of the stress level at failure, and this must also be considered. These subjects are discussed in the following paragraphs, and guidelines for specimen geometry and minimization of errors are provided.

First to be considered, however, are the merits of a four-point beam loading system as compared to the three-point beam loading system.

FOUR-POINT AND THREE-POINT LOADING

The bending moment, from which the desired fracture stress is computed in an idealized four-point beam loading system, as shown in Figure 1a, is constant, and there are no horizontal or vertical shear stresses within the inner span. However, the bending moment in an idealized three-point beam loading system, shown in Figure 2a, is linearly dependent upon the distance from the nearest support to the fracture origin, and thus requires an additional distance measurement to determine the fracture stress. Also, the shear stresses for the three-point beam loading system are developed over the full span, thus deviating from the ideally sought uniaxial stress state present in the four-point beam loading system.

Wedging stresses⁵ occur under all points of load application during flexure testing of beams. The effect of the wedging stress occurring at the inner load points of a four-point beam test is to cause a deviation from the idealized calculated constant stress at the two local regions. However, if the ratio of half the distance between the outer span L and inner span l , called a , to beam depth d is great enough,* the stress reduction will not only be small but will decay rapidly, and the stress predicted by simple beam theory will be developed. Yet, the maximum stress computed by simple beam formula for the three-point beam system is never attained. The actual maximum stress occurs at a short distance either side of the center of the load application point, which can cause fracture at these sites, rather than at the center, according to Rudnick et al.¹¹ This observation has also been confirmed by Oh and Finnie,¹² where only for a material with no scatter in strength will the fracture location of a three-point loaded beam be theoretically† located at the central load point.

Brittle materials are affected by size. Compensation can be realized through the use of statistical analysis offered by Weibull.¹³ Although the four-point beam system assures a simple stress state which is easier to analyze¹³ than the more complex biaxial stress state associated with the three-point beam specimen, this will be less of a consideration if the beam is designed properly. Nevertheless, the three-point loaded beam system is preferred when investigating material or process development, because of smaller specimen size, or when attempting to pinpoint fracture origin location.‡ On the other hand, the four-point loaded beam is preferred when determination of strength for design purposes is desired, because the center span is uniaxially stressed, i.e., no shear stresses exist. It is concluded that each of these systems is suited for a particular application and each has different advantages and disadvantages. Thus both types of loading systems, the four-point beam system shown in Figure 1 and the three-point beam system shown in Figure 2, will be considered as reference standards.

*This requirement will be discussed subsequently.

†In Reference 12, the authors considered only a statistical analysis and ignored wedging stress considerations.

‡Private communication with R. W. Rice of N. R. L.

11. RUDNICK, H., MARSHALL, C. W., DUCKWORTH, W. H., and ENRICK, B. R. *The Evaluation and Interpretation of Mechanical Properties of Brittle Materials*. AFME TR 67-316, April 1968.

12. OH, H. L., and FINNIE, I. *On the Location of Fracture in Brittle Solids - I, Due to Static Loading*. Int. J. of Fracture Mechanics, v. 6, no. 3, September 1970, p. 287-300.

13. WEIBULL, W. *Statistical Theory of Strength of Materials*. Royal Swedish Institute for Engineering Res., Proc. no. 151, 1939, p. 1-45.

Each of these beam systems will be subjected to external influences which will affect the accuracy of the test results. These external influences, directly or indirectly caused by the application of loads through the test fixtures, will lead to either configuration constraints or errors.

EXTERNAL INFLUENCES

The major influence on the accurate determination of flexure strength of a beam in bending arises from the application of load through the fixtures to the specimen. The idealizations indicated in Figures 1a and 2a are rarely met, and usually tests are conducted using a convenient rigid loading head and support member as depicted in Figures 1b and 2b. The constraints on either the loading fixture or the specimen and/or errors resulting from such fixture designs are many. Such constraints or errors, which are discussed in turn, are caused by:

1. load mislocation
2. beam twisting
3. friction
4. local stresses
5. contact point tangency shift
6. surface preparation

1. Load Mislocation

a. Four-point loaded beams

When calculating bending stress by simple beam theory formula for four-point loaded beams, it is usual to assume that the moment within the inner span ℓ is constant. However, if a loading head that can only translate is used, as idealized in Figure 1b, it is impossible to attain this idealized moment condition when $x_1 \neq x_3 - x_2$; ^{11,14} this is shown in Figure 1c. The ratio of σ_x/σ_b , from Appendix B, is:

$$\sigma_x/\sigma_b = \left[\frac{P_1}{(P_2 + P_3)/2} \right] x_1/a \quad . \quad (9)$$

The loads and distances are also shown in Figure 1c, and a is the value of a_1 with perfect load location. The error is magnified by the ratio of x_1/a . (Of course, if $P_1 = P_2 = P_3$, which implies exact location of the points of load application, there is no error.) In order to estimate the magnitude of such an error it was assumed in Appendix B that the upper two load points in Figure 1c were at a fixed distance $x_2 - x_1 = \ell$ and were constrained to translate vertically during loading, and that the loading head would be located such that $x_1 \neq x_3 - x_2$. This method of loading, being the most convenient, is usually adopted by many investigators, and therefore the resulting error determination is not unrealistic.

The analysis was accomplished by simply enforcing the condition that the displacement at x_1 must be equal to the displacement at x_2 in the deflection equation. This results in the following relationships between σ_x and σ_b in terms of the load eccentricity ratio e/L :

14. HOAGLAND, R. G., MARSHALL, C. W., and DUCKWORTH, W. H. *Reduction of Errors in Ceramic Bend Tests*. J. Amer. Cer. Soc., v. 59, no. 5-6, May-June 1976, p. 189-192.

$$\sigma_x/\sigma_b = \frac{[(e/L + a/L)/(a/L)][1-(e/L + a/L) - \ell/L]\{(\ell/L)[2-(e/L + a/L)]-2[1-(e/L + a/L)]^2\}}{3(e/L + a/L)[1- \ell/L -(e/L + a/L)]-(1- \ell/L)^2} \quad (10)$$

where the parameters a , ℓ and L are shown in Figure 1.

Most workers in the testing field utilize either a 1/3-point ($a/L = 1/3$ and $\ell/L = 1/3$) or a 1/4-point ($a/L = 1/4$ and $\ell/L = 1/2$) loading. Thus by substitution of these parameters into Equation 10, we obtain:

$$(\sigma_x/\sigma_b)_{\ell/L=1/3} = \frac{[3(e/L)+1](1/3 - e/L)[1/3(5/3 - e/L)-2(2/3 - e/L)^2]}{[3(e/L)+1](1/3 - e/L) - 4/9} \quad (11)$$

$$(\sigma_x/\sigma_b)_{\ell/L=1/2} = \frac{[4(e/L)+1](1/4 - e/L)[1/2(7/4 - e/L)-2(3/4 - e/L)^2]}{[3(e/L) + 3/4](1/4 - e/L) - 1/4} \quad (12)$$

The reader is cautioned that for given values of ℓ/L there exists a limit on e/L in (10), (11), and (12); that is, a_1 can be such that either P_2 or $P_3 = 0$ because the test system changes from four-point to an eccentric three-point loading. (See App. B.)

The error, defined as $[(\sigma_b - \sigma_x)/\sigma_x]100$, was determined from (11) and (12) for the 1/3-point and 1/4-point loaded beams and is shown in Tables 6 and 7 as a function of e/L . Even though these tables show $\pm e/L$ values, only negative values of e/L were considered in (11) and (12) because when $e/L < 0$, $\sigma_x > \sigma_b$. Tables 6 and 7 show that for corresponding e/L , when $a_1/L \neq a_2/L$, the 1/3-point loading system results in lesser error than the 1/4-point loading system. Also, in accordance with the above discussion, e/L in Tables 6 and 7 is limited to a range of ± 0.0443 and ± 0.0465 . The errors indicated in these tables can be minimized by designing the loading fixture so that the inner and outer spans are independently fixed. Also, the inner span should be designed with accurate location adjustment and allowed to pivot as recommended by Hoagland et al.¹⁴

b. Three-point loaded beams

The same type of analysis was applied to the three-point loaded beam. The ideal system is shown in Figure 2a and the system analyzed is shown in Figure 2b. The resulting percent error due to an eccentric load application is given by

$$\bar{\epsilon} = \left[(1/4) \left(\frac{1}{1-a_1/L} \right) \left(\frac{1}{a_1/L} \right) - 1 \right] 100. \quad (13)$$

The percent error as a function of e/L is given in Table 8.

Notice that the percent errors given in Table 8 are always positive, and when the load application point is misplaced, such errors are much less than those of

equivalent e/L values shown in Tables 6 and 7 for the four-point loaded beams. Notice also that when $\pm e/L = 0.500$, the error is infinite, i.e., the three-point loading model is no longer valid.

2. Beam Twisting

A net torque can result from line loads being nonuniform or nonparallel between pairs of load contact points or if the cross section of the specimen is skewed over its length.^{11,14}

Such a condition is shown schematically in Figure 3 for a four-point bending specimen. The error due to twisting has been estimated¹⁴ for both the plane stress and plane strain conditions by examining the maximum principal stress due to bending and torsion and comparing it to the bending stress. Only the details of the plane stress analysis were given in Reference 14, and bottoming of the specimen on the fixture was not considered. For the sake of completeness, the plane strain condition and bottoming are considered in the analysis given in Appendix C.

The maximum principal stress for either a skewed four-point or three-point beam in bending, considering a plane strain condition, is given by:

$$\sigma_{n_{\max}} = (\sigma_b/2)\{1+\nu+(1/3k_2)[(n/\ell'/b)^2 + 9k_2^2(1-\nu)^2]^{1/2}\} \quad (14a)$$

where σ_b is the apparent bend strength and ℓ' is either equal to "a" for four-point bending or equal to $L/2$ for three-point bending. Also:

$$n = [3k_1(E/\sigma_b)/(1+\nu)][(d/L_T)\phi_S + (d/\ell')\phi_F](b/\ell') \quad (14b)$$

where for Case I: $n = 1$, failure occurs prior to bottoming of the specimen in the loading fixture, and for Case II: $n < 1$, failure occurs after bottoming.

The factors k_1 and k_2 , obtained from Reference 2 and given in Table 9, are numerical values associated with the torsional stress component which are dependent on the ratio of b/d . The measured angle of twist (or skew angle) along the total length L_T of the specimen is ϕ_S (see Figure 3), and along the fixture from one support point to the adjacent load point, it is ϕ_F .

The maximum principal stress* as given by (14a) can be utilized to determine the percent error for various ratios of n , ℓ'/b , and b/d . This was accomplished and is shown in Table 10. Notice that the range of n varies from 0.20 to 1.00. It is expected that if bottoming does not occur prior to fracture because of an excessive twist angle, the maximum ratio of n that can be attained is 1.0 and thus the tables do not accommodate $n > 1.0$. The use of such tables is demonstrated in "Discussion of Errors."

3. Friction

It has already been shown in Table 5, for the two beam systems considered, that the error due to deflection will be equal to or less than $\frac{1}{2}\%$ if $L/d \leq 25$. It appears that these limits are well within the geometry ratios required for the reference standards to be proposed here. Therefore, friction at the load and support points will

*The maximum principal stress, assuming a plane stress condition, can be realized by simply allowing Poisson's ratio ν to be zero in Equation 14a. However, this will result in a lesser error than when assuming the plane-strain condition.

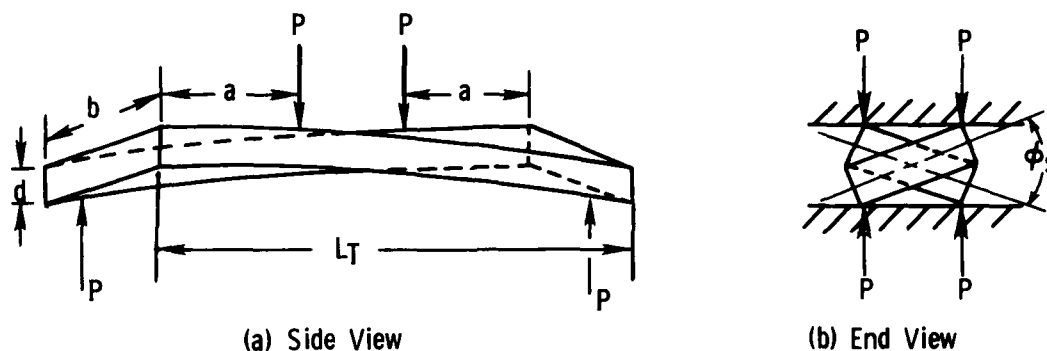


Figure 3. Twisting of a four-point beam specimen.

have a negligible effect with regard to the use of simple beam theory. This also implies that there will be no effect from friction on the contact tangency shift. (These factors will be discussed subsequently.) However, friction will cause a moment acting out of the plane of the beam that can not be ignored. This factor is considered in the following.

When determining bend strength by simple beam theory, it is usual to assume that the supports and load points are frictionless, whereas in fact they are not. The presence of friction in flexure tests with fixed load and support points gives rise to couples at such locations as well as axial forces at the neutral axis of the beam. The net axial force is relatively small and therefore is ignored here. However, if the moment is not corrected to account for the couple in the determination of flexure stress, an error will result. Error equations adapted from the results* available in the literature¹⁴⁻¹⁶ are given below for the four-point and three-point loading systems:

$$\bar{\epsilon} = 100 \left(\frac{\mu}{a/d - \mu} \right) \quad (15)$$

and

$$\bar{\epsilon} = 100 \left(\frac{\mu}{L/2d - \mu} \right) \quad (16)$$

Such errors as defined by the above equations can be significant, according to References 14, 16, and 17. Newnham¹⁶ and Weil¹⁷ reported that the experimental difference in failure stress using rigid knife edges as compared to roller-type contact points was as high as 12% for silicon nitride and 13% for graphite.

*Beam width constraint occurs also because of friction transverse to the beam's long axis. However, this effect (see Newnham¹⁶) is small and thus not considered here.

15. DUCKWORTH, W. H., et al. *Mechanical Property Tests on Ceramic Bodies*. WADC TR 52-67, March 1952, p. 67-70.

16. NEWNHAM, R. C. *Strength Tests for Brittle Materials*. Proc. of the British Cer. Soc., no. 25, May 1975, p. 281-293.

17. WEIL, N. A. *Studies of Brittle Behaviour of Ceramic Materials*. ASD TR 61-628, Part II, April 1962, p. 38-42.

4. Local Stresses

Loads on bend specimens applied through knife edges or small-diameter rollers result in high stresses under these line loads. High compressive contact stresses can result and cause local crushing. Localized contact can cause a more subtle problem, which is referred to as the wedging stress.

Also, shear stress near the locality of the load point can be several times higher than that predicted by beam theory.

a. Contact stress

Reference 5 gives equations for determining the contact pressure between a cylinder (or roller) and a flat surface (see Figure 4) as a function of the applied load, modulus of each material, and the roller radius. If it can be assumed that the two materials are identical and that the allowable bearing pressure or contact pressure can be as high as twice the bend strength of the material, then limits on the roller radius for both loading systems will result. For example, from Reference 5 we have:

$$p_{\max} = 0.59\sqrt{PE/2b\rho_1} \quad (17)$$

where p_{\max} is the maximum contact pressure. (Note that the roller radius can be either ρ_1 or ρ_2 .) However, we shall assume that $p_{\max} \leq 2\sigma_b$. Also for four-point loading, $\sigma_b = 6Pa/bd^2$, and for three-point loading, $\sigma_b = (3/2) PL/bd^2$. Substituting of σ_b into (17) and solving for ρ_1/d we obtain

$$\rho_1/d \geq 7.25/a/d, \quad \text{for the four-point loaded beam, and} \quad (17a)$$

$$\rho_1/d \geq 29.0/L/d, \quad \text{for the three-point loaded beam,} \quad (17b)$$

where it was assumed that $E/\sigma_b = 1 \times 10^3$.

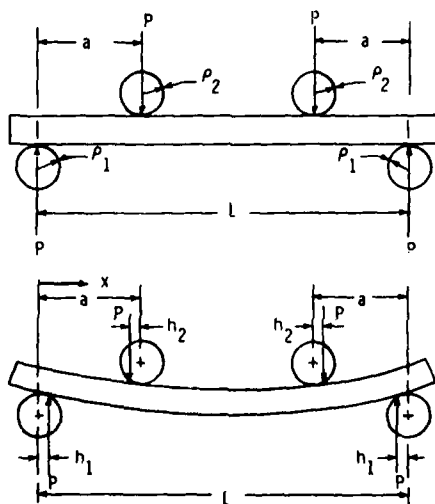


Figure 4. Contact point tangency shift.

b. Wedging stress

The effect of the wedging stress is to provide a substantial tensile stress contribution at the compressive side of the beam adjacent to the load points. A net tensile stress can not be created if $d/2\ell' < 1$, according to Reference 14. More importantly, a tensile stress is added to that already present due to beam bending at the tensile side of the beam, thereby causing a deviation from the assumed stress calculated by simple beam theory.

This problem is generally treated in Reference 2 and particular results from von Kármán and Seewald¹⁸ for a similar situation are used to estimate this error. An analysis for this error is given in Appendix D. The resulting error determination for four- and three-point loaded beams is given in Table 11. In the calculation of the errors, which are a function of a/d or L/d , as well as x'/d , the computed σ_b corresponds to the failure site location (x'/d).

c. Beam overhang

The overhangs of the beam must be great enough so that the local stresses at the beam support points are not amplified due to beam-end effects. These stresses are damped out within a distance equal to one beam depth.¹⁸ Thus, by allowing

$$L_T \geq L + 2d \quad (18)$$

we avoid beam-end effects.

d. Fracture origins

Since the contact stress is damped out with a distance d , fracture origins for the four-point loaded beam should be located within the inner span and be no closer than the beam thickness to either of the inner loading points so that test data results can be considered valid.

The distance from the closest support point to the fracture origin of a three-point loaded beam should be used to determine the moment and thus the failure stress. Also, if the failure origin is closer to either of the support points rather than the center load point, the result should be considered invalid.

5. Contact Point Tangency Shift

Significant changes in span length can occur in both four-point and three-point loading systems if contact radii of support and load points are large compared to beam depth. The shift in point of tangency, as shown by h_1 and h_2 in Figure 4, is a function of the contact radii, specimen thickness, and the ratio of the modulus of elasticity to the bend strength. For materials that behave elastically, such as those considered here, the change in tangency point and thus the error arising because of the change in moment arm from the ideal can be predicted mathematically for linear systems. This is accomplished and is presented in Appendix E. The

18. VON KÁRMÁN, T., and SEEWALD, F. *Alhandl Aerodynam, Inst. Tech. Hochschule*, 1946, p. 256.

approach was patterned after Westwater¹⁹ who corrected for span shortening but ignored friction at the support points of a three-point loaded beam.*

In Appendix E the formulas are derived for a four-point loaded beam and then reduced to the special case of a three-point loaded beam. These results are put in terms of error functions assuming the simple beam theory is applied without correcting for span shortening, as in the case of the lower support, and span lengthening between the upper loading points shown in Figure 4.

The errors are determined for four-point loaded beams of $1/3$ and $1/4$ loading points as a function of ρ_1/d and ρ_2/d , and the three-point loaded beam as a function of ρ_1/d only. It was assumed that $E/\sigma = 1 \times 10^3$. These errors are given in Table 12.

6. Surface Preparation

The flexure strength of each brittle material is not only supersensitive to the final surface finish because the maximum tensile stress occurs at the beam surface, but is also highly sensitive to prior finish history. For this reason it is impossible to specify an optimum surface finish procedure for all brittle materials, so that failure will be due to inherent flaws related to the material or material processing, rather than an imposed defect resulting from the finish process. Indeed, the designer or materials developer may not be able to specify a particular finish procedure. Therefore, rather than attempt to dictate surface finish requirements, it is suggested that each set of reported test data results be accompanied by surface finish history and/or material process history, whichever is applicable.

There are, however, several specific recommendations related to surface finishing procedures that can be presented. Corner flaws resulting from chipping or cracking during the grinding operation are sources of low-strength failure. Rounding or beveling of the corner as depicted in Figure 5 appears to reduce premature failure.²⁰ Since a chamfer will double the number of edges, thus doubling the source of flaw locations, rounding is preferred.²¹ Also, it is important to grind the edges and flat surfaces²¹ by a motion parallel to, rather than perpendicular to, the specimen length. It is further indicated²⁰ that finishing of the corner should be comparable in all aspects to that applied to the beam surfaces.

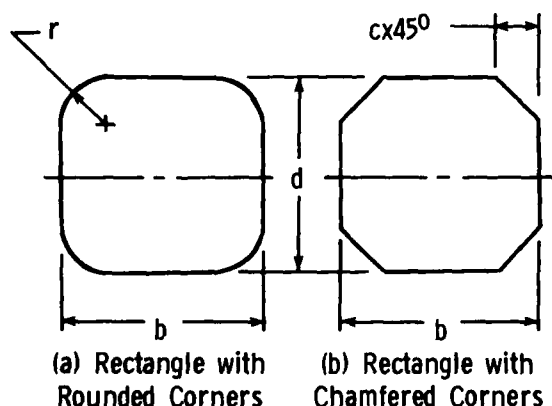


Figure 5. Beam cross section.

*Westwater also determined an approximate relationship for the horizontal load arising because of tangency shift. However, for beams of small deflection, the error is negligible.

19. WESTWATER, J. W. *Flexure Testing of Plastic Materials*. Proc. ASTM, v. 49, 1949.

20. RICE, R. W. *Machining of Ceramics*. Proc. of the Second Army Materials Technology Conference - Ceramics for High Performance Applications, J. J. Burke, A. E. Gorum, and R. N. Katz, ed., Brook Hill Publishing Company, Chestnut Hill, Massachusetts, 1974.

21. RICE, R. W. *The Effect of Grinding Direction on the Strength of Ceramics*. The Science of Ceramics Machining and Surface Finishing, S. J. Schneider and R. W. Rice, ed., NBS Special Publication 348, Washington, DC, G. P. O. (SD Cat. No. 13.10:348), 1972, p. 365-376.

If the corner radii or chamfer is small, the error in ignoring the change in moment of inertia will be negligible. The limiting ratio of corner radii or 45° chamfer dimension to beam depth can be determined from the error analysis due to neglecting the change in moment of inertia given in Appendix F. This error in determining flexure stress, when neglecting corner radii or 45° chamfer, is given in Table 13. Limiting ratio of corner radii or 45° chamfer is indicated by a line at an error level of +0.5% or less.

REFERENCE STANDARD BEAMS

Geometry Ratios

From previous discussions included under "Simple Beam Theory Assumptions" and "External Influences" a range of practical geometry ratios of b/d , a/d , L/d , and ρ_c/d can be chosen so that the error span is tolerable. This is given in Table 14, as well as the source of error. Also given in the table are the limits on roller radius to beam depth ratios so that bearing stress fracture at the contact points is precluded. The range of practical geometry ratios are $5.0 \leq a/d \leq 12.5$ for the four-point loaded beam and $20 \leq L/d \leq 25$ for the three-point loaded beam, with $b/d \leq 15.0$ and $\rho_c/d \geq 100$. These ratios were chosen to limit the accumulated error span to a reasonable total of less than approximately $\pm 2\%$. A discussion of errors considering the external influences as well will be subsequently presented.

Beam Dimensions

Most workers in the field utilize either a 1/3 or a 1/4-point loaded beam. For convenience we shall choose $L/a = 3$, because this will allow the four-point beam length to be equal to that of the three-point loaded beams.

We have already specified that $b/d \leq 15$ and we shall arbitrarily let $b/d = 2.0$ and $L/d = 21.0$. By choosing a convenient and practical beam width, such as 0.250 in. (6.35 mm), we can specify all other beam dimensions for both types of reference standard beams. These dimensions are shown in Table 15. Notice that (7) and (8) are satisfied, i.e., $L/d - a/d \leq 150$ and $L/d \leq 150$, which insures negligible nonlinear effects due to friction at the load and support points.

As indicated previously it is not the intent to require specific dimensions for the two beam systems. Indeed, this would impose a considerable waste of effort because many organizations already have a backlog data base from which test results were previously obtained from other than those beam dimensions shown in Table 15. Alternatively, it is suggested that two sets of beam dimensions indicated in the table be considered as reference bases to which other beam geometries can be related by statistical analyses. The most generally acceptable analysis appropriate to brittle materials is that conceived by Weibull.¹³ With this approach in mind, strength relationships between the reference standard beams and beams of other dimensions for volume-sensitive and surface-sensitive materials are presented in the following section. Also given is an estimate of error of the Weibull parameters as a function of sample size.

STRENGTH RELATIONSHIP AND SAMPLE SIZE

The use of beam configurations other than those recommended in Table 15 is dependent upon the establishment of a failure-strength relationship between the nonstandard and the reference standard beam. The establishment of such relationships is considered the responsibility of each investigator.

The type of analysis that has been used with varying degrees of success to relate failure strengths of brittle materials is attributed to Weibull.¹³ Many investigators have used this approach to relate strength levels of various types of specimen configurations either on a stressed volume or surface area basis.²² The reader is cautioned that confirmation of such an analysis or lack thereof may well depend on a number of factors including the test material. As examples of such correlation and lack of it, Weibull statistical correlation was justified by Davis²² for reaction-bonded silicon nitride but inappropriate for Lewis'²³ work in alumina fabricated by several processes.

A computer program for statistical evaluation of composite materials is available in Reference 24. This program determines the desirability of a particular probability density function in predicting fracture strength of ranked empirical data. The candidate functions include normal, log normal, and Weibull. Root mean square error results can be tabulated for each functional comparison. The effects of statistical ranking can be readily listed in the computer output.

The data mean and standard deviations with corresponding levels of confidence can be included in the printed results. The Weibull parameters, obtained from the maximum likelihood method, and corresponding confidence intervals can be obtained from this program.

Since a Weibull-type analysis is applicable in many instances, resulting formulas for the simple two-parameter system²⁵ to determine the risk of rupture for the four-point and three-point loading systems, are presented below, for the sake of completeness.

Volume-Sensitive Material

If the strength of material is dependent upon the volume of stressed material, the following risk-of-rupture equations are applicable for a beam stressed in pure bending* (four-point loading):

$$R_{RV} = [V_L/2(M+1)](\sigma_b/\sigma_0)^M \quad (19)$$

and for a beam stressed under three-point loading, we have:

$$R_{RV} = [V_L/2(M+1)^2](\sigma_b/\sigma_0)^M ; \quad (20)$$

where R_{RV} is the risk of rupture (volume basis). The volume for a four-point loaded beam in (19) is $V_L = 2bd$ and the volume for a three-point loaded beam in (20) is $V_L = Lbd$; also, σ_b is the mean fracture stress; σ_0 is a normalizing parameter, also called the characteristic value; and M , the Weibull slope, also called the shape parameter, is the reciprocal function of the variability of the failure stresses of the specimens in the sample. Note σ_0 has units of stress times volume ($1/M$).

M can be determined by a number of different methods (see References 22, 25, 26, and 27). The accuracy by which M can be determined is discussed later under "Weibull Parameter Estimate and Sample Size."

*Since one of the requisites for a valid test is that failure occur within the center span, only the constant moment section or pure bending form is considered for the reference standard.

22. DAVIS, D. G. S. *The Statistical Approach to Engineering Design in Ceramics*. Proc. Br. Ceramics Soc., no. 22, 1973, p. 429-452.

23. LEWIS, D., and OYLER, S. M. *An Experimental Test of Weibull Scaling Theory*. J. Amer. Cer. Soc., v. 59, no. 11-12, November-December 1976, p. 507-510.

24. AMMRC Interim Report No. 1 to MIL-HDBK 17, Composite Materials for Aircraft and Aerospace Applications (Proposed), December 1980.

25. DeSALVO, G. J. *Theory and Structural Design Applications of Weibull Statistics*. Westinghouse Astronuclear Laboratory, WANL-TME-2688, 1970.

If the average strength of a nonstandard four-point or three-point loaded beam is to be compared to that of its reference standard beam, the following relationships, obtained by simply equating the risk of rupture, are:

$$\frac{\sigma_{bNS_4}}{\sigma_{bRS_4}} = \left(\frac{V_{RS_4}}{V_{NS_4}} \right)^{1/M}, \text{ and } \frac{\sigma_{bNS_3}}{\sigma_{bRS_3}} = \left(\frac{V_{RS_3}}{V_{NS_3}} \right)^{1/M} \quad (21)$$

where $\sigma_{bNS_{4,3}}$ and $\sigma_{bRS_{4,3}}$ are the average fracture stress in bending of a nonstandard and reference standard beam, and $V_{NS_{4,3}}$ and $V_{RS_{4,3}}$ are the volumes of the four-point or three-point loaded nonstandard and reference standard beams, i.e., $V_{RS_4} = lbd$ or $V_{RS_3} = Lbd$.

If the average strength of the reference standard three-point loaded beam is to be compared to the reference standard four-point loaded beam, then

$$\sigma_{bRS_3}/\sigma_{bRS_4} = [(1/3)(M+1)]^{1/M}; \quad (22)$$

note

$$V_{RS_4}/V_{RS_3} = 1/3.$$

Surface-Sensitive Material

If the strength of the material is dependent upon the surface-stressed material, the following general risk-of-rupture equations²⁵ are applicable for a rectangular beam stressed by pure bending (four-point loading):

$$R_{RS} = \frac{A_L}{2(M+1)} \left(\frac{1}{M+1} + \lambda \right) \left(\frac{\sigma_b}{\sigma_o} \right)^{M_s} \quad (23)$$

and a beam stressed by three-point loading:

$$R_{RS} = \frac{A_L}{2(\lambda+1)(M+1)} \left(\frac{1}{M+1} + \lambda \right) \left(\frac{\sigma_b}{\sigma_o} \right)^{M_s} \quad (24)$$

where R_{RS} is the risk of rupture (surface basis); λ is defined as b/d ; A_L in (23) is defined as $2l(b+d)$; A_L in (24) is defined as $2L(b+d)$; and M_s is the Weibull slope parameter for a surface-sensitive material.

The Weibull slope parameter for the surface material in general is not the same as that for the interior material. According to Paluszny and Wu²⁷ these differences can be minimized by improving surface finishes. Regardless, for such a case, (19) and (20) are still applicable.

26. McLEAN, A. F., and FISHER, E. A. *Brittle Materials Design. High Temperature Gas Turbine*. Ford Motor Company, Contract DAAG46-71-C-0162, Interim Report, AMMRC CTR 77-20, August 1977.

27. PALUSZNY, A., and WU, W. *Probabilistic Aspects of Designing with Ceramics*. Presented at the 22nd Annual Gas Turbine Conference of A.S.M.E., Philadelphia, Pennsylvania, March 27-31, 1977.

However, if the average strength of a nonstandard four-point or three-point loaded beam, sensitive to surface area, is to be compared to that of its reference standard beam, the following relationships are appropriate:

$$\frac{\sigma_{bNS_4}}{\sigma_{bRS_4}} = \left\{ \left(\frac{ARS_4}{ANS_4} \right) \left(\frac{1/(M+1) + \lambda_{RS_4}}{1/(M+1) + \lambda_{NS_4}} \right) \right\}^{1/M_s}, \text{ and} \quad (25)$$

$$\frac{\sigma_{bNS_3}}{\sigma_{bRS_3}} = \left\{ \left(\frac{ARS_3}{ANS_3} \right) \left(\frac{\lambda_{NS_3} + 1}{\lambda_{RS_3} + 1} \right) \left(\frac{1/(M+1) + \lambda_{RS_3}}{1/(M+1) + \lambda_{NS_3}} \right) \right\}^{1/M_s},$$

where $ANS_{4,3}$ and $ARS_{4,3}$ are surface areas of the four-point or three-point loaded nonstandard and reference standard beams, i.e., $ARS_4 = 2l(b+d)$ and $ARS_3 = 2L(b+d)$ where $\lambda_{NS_{4,3}}$ and $\lambda_{RS_{4,3}}$ are the width-to-height ratio of the nonstandard and reference standard beams.

Weibull Parameter Estimate and Sample Size

Flexure tests on hot-pressed silicon nitride material reported by McLean and Baker²⁸ show the effect of Weibull slope M for specific component reliability. The strength requirement for a specific component reliability was decreased 16% by a reported 20% increase in M from a nominal value of 10, and was increased 27% by a 20% decrease in the slope.

Different techniques will produce somewhat different results, according to McLean and Fisher,²⁶ when estimating the Weibull parameters. Two statistical methods had been used during preliminary analysis of hot-pressed silicon nitride material strength data, and results indicated that the estimate of the characteristic value σ_0 (or scale parameter) were very close while the Weibull slope estimates vary and thus would yield considerable differences in the component strength requirement.

The following is quoted directly from Reference 26 (except to change reference and figure numbers appropriate for this report) because it succinctly addresses the answer to the question of proper sample size: "The exact confidence intervals for the parameters are based on the distributions obtained by Monte Carlo methods presented in Thoman et al.²⁹ It is not unexpected that the uncertainty in the estimation of a parameter will increase as the sample size decreases. This uncertainty, however, has rarely been quantified. The width of the confidence intervals for the parameters is a measure of the uncertainty and aids in the selection of the sample size of a test. Figures 6 and 7 are drawn from Reference 29 and show the 90% confidence bounds for the Weibull slope and the characteristic value." (Figure 7 differs from that given in Reference 26 in that two additional M values were computed and shown.) "The bounds for the Weibull slope are a function of sample size only, while for the characteristic value they are a function of both the sample size and the Weibull slope. As can be seen from the graphs, the error or uncertainty in estimates from small sample sizes is very large. Important judgements and significant analysis should not be based on small samples. Sample sizes of at least 30 should be used for all but the most preliminary investigations. An uncertainty of $\pm 10\%$ in Weibull slope requires more than 120 samples. This uncertainty is not peculiar to just ceramics, but is intrinsic to the statistical analysis of data, whether that data be material strength or the life

28. McLEAN, A. F., and BAKER, R. R. *Brittle Materials Design, High Temperature Gas Turbine*. Ford Motor Company, Contract DAAG46-71-C-0162, Interim Report, AMMRC CTR 76-31, October 1976.

29. THOMAN, D. R., BAIN, L. J., and ANTLE, C. E. *Inferences on the Parameters of Weibull Distribution*. Technometrics, v. 11, August 1969, p. 445-460.

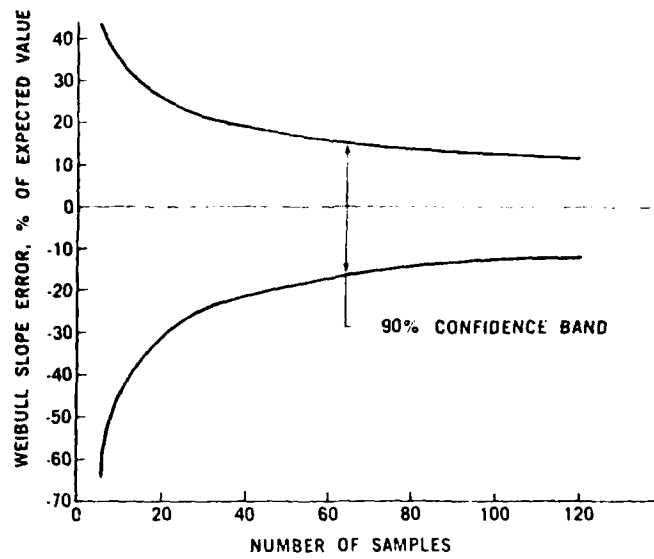


Figure 6. Weibull slope error versus sample size.

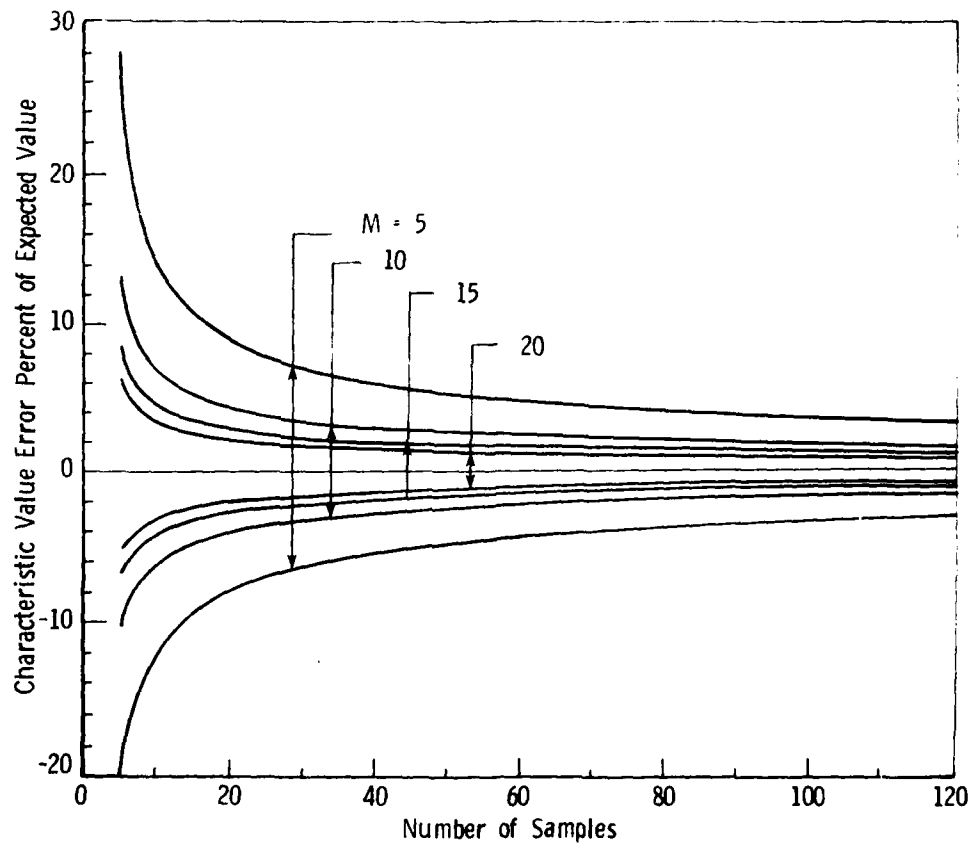


Figure 7. Characteristic value error versus sample size - 90% confidence bands.

of some electronic component. The choice of sample size depends on many factors including the cost and timing of testing and the degree of conservation which is acceptable, but erroneous judgements may be made and unacceptable designs pursued if the sample sizes are too small."

LOADING SPEED

It is well known that brittle materials are strain-rate sensitive, and thus speed of loading will influence the stress at which failure of the beam will occur. To choose a "static" speed which would insure no strain-rate effect for all brittle materials would not only be impossible but time consuming when testing those materials that exhibit a lesser strain-rate effect. However, most materials testing facilities utilize an Instron testing machine. Normally the slowest test speed in such a machine is 0.02 in./min (0.51 mm/min). It would seem appropriate, therefore, to utilize this speed of testing in conjunction with the two reference standard beams given in Table 15 to establish a reference standard strain-rate. This is accomplished in the following for both the 1/3-four-point and three-point loaded beams.

The strain rate is defined as:

$$\dot{\epsilon} = (\sigma_b/E)/t, \quad (26)$$

where t is the time of the applied load; but since the speed of loading is $s=y/t$, then

$$\dot{\epsilon} = (\sigma_b/E)/ys \quad (27)$$

where y is the deflection of the beam and s is the constant speed of the testing machine.

The deflection at the center of a four-point loaded beam is:

$$y = (Pa/24EI)(3L^2-4a^2) \quad (28)$$

Recalling that $Pa = 2\sigma_b I/d$, and substitution of this and (28) into (27) gives:

$$\dot{\epsilon} = \frac{12ds}{3L^2-4a^2} \quad (29)$$

for the four-point loaded beam.

For the 1/3-four-point loaded beam, where $a=L/3$, we obtain:

$$\dot{\epsilon} = (108/23)(d/L^2)s \quad (30)$$

Using the same approach as above, we obtain the strain rate for the three-point loaded beam as:

$$\dot{\epsilon} = (6d/L^2)s \quad (31)$$

With a loading speed of 0.02 in./min (0.51 mm/min) or 333×10^{-6} in./sec (8458×10^{-6} mm/sec), we obtain strain rates of 28×10^{-6} /sec for the 1/3-four-point reference standard beam (29) and 36×10^{-6} /sec for the three-point reference standard beam (31). These strain rates shall be considered as reference standards for both beam systems as indicated in Table 15.

DISCUSSION OF ERRORS

The errors associated with flexure testing of beams can be classified according to their source, i.e., related to the use of simple beam theory (beam dimensions) or sources arising from external load applications. Table 16 lists the sources and summarizes the error span for the first category and Table 17 for the second.

Table 16 shows resulting error spans of -0.4% to +0.3% for both the 1/3-four-point reference standard beam and the three-point reference standard beam geometries described in Table 15. These errors, as expected, are rather small.

The errors summed in Table 17 are not of small magnitude and require some explanation. These are discussed in the order in which they appear.

Error Due to Load Mislocation

In the calculation of the error associated with load mislocation, it was assumed that loading heads and supports are rigid, can not rotate (see Figures 1b and 2b), and are located manually. Thus it is also assumed that the best possible location tolerance that can be obtained is $\pm 1/64$ in. (0.40 mm). The errors due to load mislocation were determined by interpolation from Tables 6 and 8 with $e/L = \pm 0.006$.

Error Due to Beam Twisting

Again it is assumed that the loading heads and supports are designed as indicated in Figures 1b and 2b. Thus, twisting of the specimen can occur due to nonparallel pairs of load or support points and specimen skewness, as schematically indicated in Figure 3. Table 10 allows the error determination caused by such undesirable action. We shall determine the error for both reference standard specimens given in Table 16 with an assumed but realistic set of test parameters and test results for illustrative purposes.

It will be assumed that the material is hot-pressed silicon nitride with $E = 45 \times 10^6$ psi, and $\nu = 0.25$. The bend strength determined during the test for the 1/3-four-point loaded beam was 60×10^3 psi, and for the three-point loaded beam was 67×10^3 psi. The measured angle of twist of the specimen configurations is assumed to be small with respect to that of the loading fixtures. It is assumed that the best alignment of the loading fixtures with each other will be no less than 1.0° ; thus $\phi_S \approx 0$ and $\phi_F = 1^\circ$.

In order to utilize Table 10, we must first determine n ; recalling equation 14b:

$$n = [3k_1(E/\sigma_b)/(1+\nu)][(d/L_T)\phi_S + (d/\ell')\phi_F](b/\ell') .$$

Since $b/d = 2.0$, then k_1 from Table 9 is 0.229; for the 1/3-four-point loaded beam, $d/L_T = 0.043$, $d/\ell' = 0.143$, and $b/\ell' = 0.286$. Thus, n according to the above relationship is approximately 0.4. Utilizing Table 10b, with $b/d = 2.0$ and $\ell'/b = 3.50$, by linear interpolation we determine the error to be -1.0%. For the three-point loaded beam, $d/L_T = 0.043$, $d/\ell' = 0.095$, and $b/\ell' = 0.190$; and n , calculated from the above relationship, is approximately equal to 0.2. Entering Table 10a and interpolating with $b/d = 2.0$ and $\ell'/b = 5.25$, we determine the error to be approximately -0.1%.

Note that in the above example, $n < 1.0$, indicating that failure occurs after bottoming. If n had been greater than 1.0, i.e., no bottoming prior to failure, then Table 10e would have been used to calculate the error.

Error Due to Friction

If moveable roller contact points are not used in the load and support fixtures, an error in determining the flexure stress at failure will result. An estimate of the coefficient of friction obtained¹⁶ by comparing fracture strengths when using rigid as compared to roller-type contacts was determined to be 0.4 for silicon nitride material. This value was also obtained in Reference 15 for hard steel on garnet and Reference 17 for steel on graphite. Using equations 15 and 16, the errors as indicated in Table 17 are +6.1% for the four-point beam and +4.0% for the three-point beam.

Error Due to Wedging Stress

Since a/d for the four-point reference standard beam is 7 and L/d is 21 for the three-point reference standard beam, then, from Tables 11a and 11b, assuming the maximum error can occur, i.e., $x' = 0$, the respective errors are +0.7% and +0.9%.

Error Due to Contact Point Tangency Shift

There are two conflicting requirements regarding contact radius at the loading and support points: the first is that radii must be great enough so that contact or bearing pressure does not cause local failure of the beam, and the second is that the contact radii be small enough so that the error due to contact point tangency shift is not great.

Equations 17a and 17b allow the determination of the radii such that the contact pressure is not excessive. Since we have allowed the contact radius to beam thickness ratio to be 1.5 ($\rho_1/d = \rho_2/d = \rho/d = 1.5$) for both reference standard beam systems, equations 17a and 17b are both satisfied, and the resulting radius of 3/16 inch (4.76 mm) is of practical size. The errors due to contact point tangency shift, +0.5% and +0.2% were then obtained from Tables 12a and 12c for the four-point and three-point beam systems.

Corner Radii

The error when ignoring corner radii in determining the flexure stress at failure and neglecting the change in the moment of inertia with $b/d = 2.0$ and $r/d = 0.06$ is +0.4% for both systems as obtained from Table 13.

It is noted that three error sources associated with the determination of flexure stress at failure, not included in Table 17 because they are intrinsic to the material, are unequal Young's moduli (Table 2), anisotropy, and nonhomogeneity. Each investigator will have to establish if these factors are present, and if so, their magnitudes.

Error Span Summary

The error spans indicated in Table 17 for the four-point and three-point beam reference standard systems are -5.0% to +7.7% and -0.1% to +5.6%. Adding those given in Table 16 results in a total of -5.4% to +8.0% and -0.5% to +5.9%. The three-point loaded beam has a lower error span associated with it than the four-point loaded beam because of lesser inherent errors in load mislocation, beam twisting, friction at the load and support contact points, and contact point tangency shift. For the four-point loaded beam, the two major sources of error are caused by load mislocation and friction, which can be reduced to a great degree by proper design. If these two sources of error could be minimized (assumed to be zero), the total error spans would be

reduced to -1.0% to +1.6%. The major source of error for the three-point beam in bending is due to friction and if eliminated would result in a total error span of -0.1% to +1.6%.

These minimized total error spans are attainable by designing load and support fixtures that incorporate rolling contacts and pivot in the two required directions, i.e., about the beam axis and transverse to it. Such loading systems have been designed¹⁴ and extensively used in practice.*

RECOMMENDATIONS AND CONCLUSIONS

1. The recommended beam configurations, called reference standards, are 1/3-four-point and three-point loaded beams having the following dimensions (see Figures 1a and 2a):

- $b = 0.250$ inch (6.35 mm)
- $d = 0.125$ inch (3.18 mm)
- $a = 0.875$ inch (22.23 mm)
- $L = 2.625$ inch (66.68 mm)
- $L_T \geq 2.875$ inch (73.03 mm)
- $r \geq 0.008$ inch (0.20 mm)

2. The recommended contact radius used in both the loading and support fixtures is 0.1875 inch (4.76 mm).

3. The errors due to simple beam theory assumptions for the reference standard beams are relatively small.

4. The total estimated error spans for the above beam dimensions are -5.4% to +8.0% for the 1/3-four-point beam and -0.5% to +5.9% for the three-point beam. Not included in these error spans are the intrinsic effects of unequal Young's modulus, anisotropy, and nonhomogeneity of the beam material.

5. If a properly designed fixture is utilized during testing of the four-point loaded reference standard beam, such that errors due to an assumed $\pm 1/64$ -inch load mislocation and an assumed 1° twisting angle of the loading fixtures are eliminated, as well as eliminating a coefficient of friction of 0.4, then the error span is reduced accordingly from -1.0% to +1.6%.

6. The major source of error associated with the reference standard three-point loaded beam is due to friction at the support and load points; elimination of this results in an error span of -0.1% to +1.6%.

7. It is recommended that the load and supporting fixtures for both reference standard systems be designed so that:

- a. the load and support points be accurately fixed and known; and
- b. friction be minimized at the load and support points through the use of freely pivoting rollers or by other means.

*Private communications with L. Gibson of Carborundum Co., W. Duckworth of Battelle Columbus Laboratories, and J. Caverly of Ford Motor Company.

8. In addition to item 7 above, the reference standard four-point-beam system employs load fixtures that are free to pivot in two mutually perpendicular directions. Although two beam systems are recommended and referred to as reference standards, other systems are acceptable as long as strength relationships through proven statistical analyses are insured, and the errors associated with the beam and loading geometry (obtainable from the tables in the text) are estimated and reported along with the strength data.

9. A minimum reference standard sample size of 30 is recommended. This will result in an error of approximately $\pm 25\%$ in the determination of the Weibull slope parameter M within a 90% confidence band (see Figure 6). Such a sample size will result in error, dependent on M , obtained from Figure 7 in the determination of the characteristic value σ_0 ; this error should be reported also. If the minimum sample size can not be realized, the errors in determining M and σ_0 should be reported along with the test results.

10. No specific surface finishing procedure is recommended but this will be considered the responsibility of the individual investigator. Nevertheless, each set of test results should include surface finish or material process history, whichever is applicable. Surface preparation parallel to the beam's long axis is recommended, and should include rounding or beveling of the beam edges. Rounding of the edges is preferred, but both are acceptable.

11. If the fracture origins in four-point loaded beams can be determined, they must be located within the inner span and be no closer than the beam thickness to the load points in order that test data results be considered valid.

12. The distance from the closest support point to the fracture origin of a three-point loaded beam must be measured and used in computing the moment and resulting bending stress. Also, if the failure origin is closer to either of the outer support points than the central loading point, the results can be considered invalid.

13. The reference standard test speed of loading should be 0.02 inch/minute (0.52 mm/min). This results in a strain rate of 28×10^{-6} /sec for the reference standard 1/3-four-point beam system and 36×10^{-6} /sec for the three-point beam systems. If any other speed of loading is used, it should be reported.

14. It is further recommended that accurate analyses of the following problems as related to brittle materials be accomplished:

- a. Exact stress distribution for four-point and three-point loaded beams so that a more accurate error analysis than that given in Table 1 be realized.
- b. The stress distribution for parabolic nonhomogeneous material for four-point and three-point loaded beams such that realistic errors may be obtained for a varying modulus of elasticity as a function of beam depth.
- c. Anisotropy be accounted for when determining bend strength.

15. Finally, it is suggested that a simple and easy-to-use loading fixture, as suggested in recommendations 7 and 8 above, be developed, if feasible.

TABULATIONS OF ERRORS IN CALCULATING FLEXURE STRESS

Unless otherwise stated, the percent error is determined throughout the text as $[(\sigma_b - \sigma_x)/\sigma_x]100$; where $\sigma_b = 6M/bd^2$ and σ_x is more nearly the true bending stress.

Table 1. ERROR DUE TO NON-LINEAR STRESS DISTRIBUTION

a/d or L/d	% Error
0	100
0.5	51.6
0.75	32.2
1.0	21.1
1.5	10.6
2.0	6.2
2.5	4.1
3.0	2.9
3.5	2.1
4.0	1.6
4.5	1.3
5.0	1.1
6.0	0.7
8.0	0.4
10.0	0.3
∞	0

Note: All errors are negative.

Table 2. ERROR WHEN $E_T \neq E_C$

E_T/E_C	% Error	E_T/E_C	% Error
0.20	+38.2	1.025	-0.6
0.40	+22.5	1.050	-1.2
0.60	+12.7	1.075	-1.8
0.80	+5.6	1.10	-2.4
0.90	+2.6	1.15	-3.5
0.925	+1.9	1.20	-4.6
0.950	+1.3	1.30	-6.5
0.975	+0.6	1.40	-8.4
1.00	0	1.60	-11.7
		1.80	-14.6
		2.0	-17.2

Table 3. ERROR CAUSED BY INITIAL BEAM CURVATURE

ρ_c/d	% Error
1	35.1
2	16.7
3	10.9
4	8.4
10	3.2
15	2.2
20	1.7
40	0.8
100	0.3
$\epsilon = 100 [(\alpha_b - \alpha_c)/\alpha_c]$	

Note: All errors are negative.

Table 4. ERROR CAUSED BY EFFECT OF ANTICLASTIC CURVATURE

$E/\sigma_b = 1 \times 10^3$	
b/d	% Error
1.0	0
15.0	0
20.0	0.1
30.0	0.6
40.0	1.5
50.0	2.6
100.0	4.7
500.0	5.9
1000.0	6.1
∞	$+ (-v^2)100 = -6.25\%$

Note: All errors are negative.

Table 5. ERROR FOR BEAMS WITH LARGE DEFLECTION

$E/\sigma_b = 0.5 \times 10^3$			
% Error Beam Loading			
L/d	1/3-Four-Point	1/4-Four-Point	Three-Point
0	0	0	0
25	0.4	0.5	0.3
50	0.9	1.1	0.7
100	2.0	2.3	1.5
150	2.8	3.2	2.1
250	6.3	7.1	4.7

Note: All errors are positive.

Table 6. ERROR DUE TO ECCENTRIC LOAD APPLICATION FOR A 1/3-FOUR-POINT LOADED BEAM

When $e/L = 1/3$ and $a_1/L \neq a_2/L$	
$e/L = \pm(a_1/L - 1/3)$	% Error
0	0
0.0019	1.0
0.0038	2.6
0.0057	3.8
0.0076	4.9
0.0095	6.0
0.0114	7.0
0.0133	8.1
0.0333	16.1
0.0433	18.7
0.0443	18.9

Note: All errors are negative.

Table 7. ERROR DUE TO ECCENTRIC LOAD APPLICATION FOR A 1/4-FOUR-POINT LOADED BEAM

When $e/L = 1/2$ and $a_1/L \neq a_2/L$

$e/L = \pm(a_1/L - 1/4)$	% Error
0	0
0.0040	3.8
0.0080	7.1
0.0120	10.0
0.0160	12.6
0.0200	14.7
0.0240	16.6
0.0280	18.3
0.0320	19.8
0.0340	20.8
0.0400	21.8
0.0465	22.9

Note: All errors are negative.

Table 8. ERROR DUE TO ECCENTRIC LOAD APPLICATION FOR A THREE-POINT LOADED BEAM

When $a_1/L \neq a_2/L \neq 1/2$
 $e/L = 1/2 - a_1/L$

$\pm e/L$	% Error
0	0
0.025	0.25
0.050	1.0
0.075	2.3
0.100	4.2
0.150	9.9
0.200	19.0
0.250	33.3
0.300	56.3
0.400	177.8
0.450	426.3
0.500	∞

Note: All errors are positive.

Table 9. k_1 AND k_2

b/d	k_1	k_2
1.0	0.1406	0.208
1.2	0.166	0.219
1.5	0.196	0.231
2.0	0.229	0.246
2.5	0.249	0.258
5.0	0.291	0.291
10.0	0.312	0.312
∞	0.333	0.333

Table 10. % ERROR DUE TO BEAM TWISTING
 $\nu = 0.25$

		b/d							
		1.00	1.2	1.5	2.0	2.5	5.0	10.0	∞
a. $n = 0.20$	1.0	3.18	2.88	2.61	2.32	2.12	1.68	1.47	1.30
	2.0	0.84	0.76	0.68	0.60	0.55	0.43	0.38	0.33
	2.5	0.54	0.49	0.44	0.39	0.35	0.38	0.24	0.21
	5.0	0.14	0.12	0.11	0.10	0.09	0.07	0.06	0.05
	10.0	0.03	0.03	0.03	0.02	0.02	0.02	0.02	0.10
	∞	0	0	0	0	0	0	0	0
b. $n = 0.40$	1.0	10.58	9.77	8.94	8.06	7.44	6.05	5.36	4.77
	2.0	3.18	2.89	2.61	2.32	2.12	1.68	1.47	1.30
	2.5	2.09	1.89	1.71	1.51	1.38	1.09	0.95	0.84
	5.0	0.54	0.49	0.44	0.39	0.35	0.28	0.24	0.21
	10.0	0.14	0.12	0.11	0.10	0.09	0.07	0.06	0.05
	∞	0	0	0	0	0	0	0	0
c. $n = 0.60$	1.0	19.01	17.75	16.51	15.11	14.11	11.79	10.58	9.54
	2.0	6.58	6.02	5.48	4.70	4.50	3.61	3.18	2.81
	2.5	4.44	4.04	3.67	3.26	2.99	2.38	2.09	1.84
	5.0	1.20	1.08	0.98	0.86	0.77	0.62	0.54	0.48
	10.0	0.31	0.28	0.25	0.22	0.20	0.16	0.14	0.12
	∞	0	0	0	0	0	0	0	0
d. $n = 0.80$	1.0	26.88	25.38	23.86	22.12	20.86	17.92	16.22	14.79
	2.0	10.58	9.75	8.94	8.06	7.44	6.09	5.36	4.77
	2.5	7.35	6.73	6.14	5.50	5.05	4.09	3.58	3.17
	5.0	2.09	1.89	1.71	1.51	1.38	1.10	0.95	0.84
	10.0	0.54	0.49	0.44	0.39	0.35	0.28	0.24	0.21
	∞	0	0	0	0	0	0	0	0
e. $n = 1.00$	1.0	33.75	32.13	30.47	28.54	27.11	23.64	21.73	20.03
	2.0	14.80	13.74	12.69	11.53	10.71	8.83	7.87	7.05
	2.5	10.58	9.75	8.94	8.06	7.44	6.05	5.36	4.77
	5.0	3.18	2.89	2.61	2.32	2.12	1.68	1.47	1.30
	10.0	0.84	0.76	0.68	0.60	0.55	0.43	0.38	0.33
	∞	0	0	0	0	0	0	0	0

Note: All errors are negative.

Table 11. ERROR DUE TO WEDGING

Loading	x'/d^*							
	0	0.125	0.25	0.375	0.50	0.75	1.0	1.50
a. Four-point								
a/d								
1.0	4.7	-0.5	-2.8	-2.1	-1.4	-0.7	-0.3	0
1.5	+3.1	-0.3	-1.9	-1.4	-0.9	-0.5	-0.2	0
2.0	+2.3	-0.2	-1.4	-1.1	-0.7	-0.4	-0.2	0
3.0	+1.5	-0.2	-1.0	-0.7	-0.5	-0.2	-0.1	0
4.0	+1.1	-0.1	-0.7	-0.5	-0.3	-0.2	-0.1	0
5.0	+0.9	-0.1	-0.6	-0.4	-0.3	-0.1	0	0
6.0	+0.8	-0.1	-0.5	-0.4	-0.2	-0.1	0	0
8.0	+0.6	0	-0.4	-0.3	-0.2	-0.1	0	0
10.0	+0.4	0	-0.3	-0.2	-0.1	-0.1	0	0
15.0	+0.3	0	-0.2	-0.1	-0.1	0	0	0
20.0	+0.2	0	-0.1	-0.1	-0.1	0	0	0
40.0	+0.1	0	-0.1	-0.1	0	0	0	0
60.0	+0.1	0	0	0	0	0	0	0
∞	0	0	0	0	0	0	0	0
Three-point								
L/d								
1.0	+21.6	-2.4	-18.8	-25.4	-100.0	+6.2	+1.3	0
1.5	+13.4	-1.4	-10.4	-10.2	-10.1	-100.0	+2.6	0
2.0	+9.7	-1.0	-7.2	-6.4	-5.3	-5.5	-100.0	+0.1
3.0	+6.3	-0.7	-4.4	-3.7	-2.7	-1.9	-1.3	-100.0
4.0	+4.7	-0.5	-3.2	-2.6	-1.8	-1.2	-0.6	-0.1
5.0	+3.7	-0.4	-2.5	-2.0	-1.4	-0.8	-0.4	0
6.0	+3.1	-0.3	-2.1	-1.6	-1.1	-0.6	-0.3	0
8.0	+2.3	-0.2	-1.5	-1.2	-0.8	-0.4	-0.2	0
10.0	+1.8	-0.2	-1.2	-0.9	-0.6	-0.3	-0.2	0
15.0	+1.2	-0.1	-0.8	-0.6	-0.4	-0.2	-0.1	0
20.0	+0.9	-0.1	-0.6	-0.4	-0.3	-0.2	-0.1	0
40.0	+0.4	0	-0.3	-0.2	-0.1	-0.1	0	0
60.0	+0.3	0	-0.2	-0.1	-0.1	-0.1	0	0
∞	0	0	0	0	0	0	0	0

is the distance on either side of the load contact point where failure occurs.

Table 12. % ERROR DUE TO TANGENCY POINT SHIFT

$$E/\sigma_b = 1 \times 10^3$$

Loading	ρ_1/d	ρ_2/d			
		1.0	2.0	5.0	10.0
a. Four-point, $a/L = 1/3$	1.0	0.3	0.4	0.7	1.2
	2.0	0.5	0.6	0.9	1.4
	4.1	0.9	1.0	1.3	1.8
	6.1	1.3	1.4	1.7	2.3
	8.2	1.7	1.8	2.1	2.7
	10.3	2.1	2.2	2.6	3.1
b. Four-point, $a/L = 1/4$	0.67	0.4	0.6	1.2	2.2
	1.35	0.6	0.8	1.4	2.5
	2.7	1.0	1.2	1.8	2.9
	4.1	1.4	1.6	2.2	3.3
	5.5	1.8	2.0	2.6	3.7
	6.9	2.2	2.4	3.1	4.1
c. Three-point, $a/L = 1/2$	1.0	0.1	Regardless of ρ_2/d value		
	2.0	0.2			
	4.0	0.4			
	6.0	0.6			
	8.0	0.8			
	10.0	1.0			

Note: All errors are positive.

Table 13. % ERROR IN DETERMINING FLEXURE STRESS

a. When neglecting corner radii	r/d	b/d		
		1.0	2.0	4.0
	0	0	0	0
	0.02	0.1	0.1	0
	0.04	0.4	0.2	0.1
	0.06	0.9	0.4	0.2
	0.08	1.5	0.8	0.4
	0.10	2.4	1.2	0.6
	0.15	5.4	2.6	1.3
	0.20	9.7	4.6	2.2

b. When neglecting 45° chamfer	c/d	1.0	2.0	4.0
		1.0	2.0	4.0
	0	0	0	0
	0.01	0.1	0.1	0.1
	0.02	0.2	0.1	0.1
	0.03	0.5	0.3	0.1
	0.04	0.9	0.5	0.2
	0.05	1.4	0.7	0.4
	0.06	2.0	1.0	0.5
	0.08	3.4	1.7	0.9
	0.10	5.2	2.6	1.3

Note: All errors are positive.

Table 14. SOURCES AND ERRORS

Error Source	Four-Point				Three-Point			
	a/d	$\bar{\epsilon}$	ρ_1/d	$\bar{\epsilon}$	L/d	$\bar{\epsilon}$	ρ_1/d	$\bar{\epsilon}$
Nonlinear Stress Distribution, (Table 1)	≥ 3.5	≤ -2.1	-	-	≥ 7.0	≤ -0.6	-	-
$E_t \neq E_c$, (Table 2) Nonhomogeneity and Anisotropy	Error Dependent Upon Material and/or Fabrication Process							
Initial Beam Curvature, (Table 3)	$\rho_c/d \geq 100$, $\bar{\epsilon} \leq -0.3$							
Anticlastic Curvature,* (Table 4)	$b/d \leq 15$, $\bar{\epsilon} = 0$							
Large Deflection, (Table 5)	≤ 12.5	$+0.3$	-	-	≤ 25	$\leq +0.3$	-	-
Wedging Stress,** (Table 11)	≥ 5 (Table 11a)	≤ -0.9	-	-	≥ 20 (Table 11b)	$\leq +0.9$	-	-
Tangency Point Shift	-	-	$\leq 1.5^+$ (Table 12a, $a/L = 1/3$)	$\leq +0.5$	-	-	≤ 1.5 (Table 12c)	$\leq +0.2$
Neglecting Corner Radii or Chamfer (Table 13)	$r/d \leq 0.06$ $c/d \leq 0.04$				$\bar{\epsilon} \leq +0.5$			
Contact Stress	-	-	$\geq 7.25/(a/d)$ (Eq. 17a)	-	-	-	$\geq 29.0/(L/d)$ (Eq. 17b)	-

*Assumed $E/\sigma_b = 1 \times 10^3$ **Assumed the most conservative case ($x' = 0$).†Assumed $\rho_1/d = \rho_2/d$ for both beam systems.

Table 15. REFERENCE STANDARD BEAM SYSTEMS

	1/3-Four-Point Beam		Three-Point Beam
b/d	2.0		2.0
a/d	7.0		10.5
L/d	21.0		21.0
ρ_1/d	1.5		1.5
d/L _T	0.043 in.	(1.104 mm)	0.043 in.
b	0.250 in.	(6.350 mm)	0.250 in.
d	0.125 in.	(3.175 mm)	0.125 in.
a	0.875 in.	(22.225 mm)	1.313 in. (32.944 mm)
r	0.008 in.	(0.203 mm)	0.008 in.
or c	0.005 in.	(0.127 mm)	0.005 in.
ϵ	0.875 in.	(22.225 mm)	-
L	2.625 in.	(66.675 mm)	2.625 in.
L _T	2.875 in.	(73.025 mm)	2.875 in.
ρ_1	0.1875 in.	(4.763 mm)	0.1875 in.
s	0.02 in./min	(0.508 mm/min)	0.02 in./min
$\dot{\epsilon}$	$28 \times 10^{-6}/\text{sec}$		$36 \times 10^{-6}/\text{sec}$

Table 16. % ERRORS DUE TO SIMPLE BEAM THEORY ASSUMPTIONS APPLIED TO REFERENCE STANDARD BEAM TYPE LOADING

Source	1/3-Four-Point and Three-Point Loading
Nonlinear Stress Distribution, L/d=21, Table 1	-0.1
Beam Curvature, $\rho_C \geq 100$, Table 3	-0.3
Anticlastic Curvature, b/d = 2, Table 4	0
Large Deflection,* L/d = 21, Table 5	+0.3
Error Span due to Beam Geometry	-0.4 to +0.3

*Assumed $E/\sigma_b = 0.5 \times 10^3$

Table 17. % ERRORS CAUSED BY EXTERNAL FACTORS FOR REFERENCE STANDARD BEAMS

Source	Type of Loading	
	1/3-Four-Point	Three-Point
Load Mislocation $e/L = \pm 0.006$	-4.0 (Table 6)	+0.1 (Table 8)
Beam Twisting, Table 10 ($\phi_s = 0$, $\phi_F = \frac{1}{2}^\circ$)	-1.0	-0.1
Friction ($\mu = 0.4$)	+6.1 (Eq. 15)	+4.0 (Eq. 16)
Wedging*	+0.7 (Table 11a)	+0.9 (Table 11b)
Contact Point Tangency Shift,	$\approx +0.5$ $\rho_1/d = \rho_2/d = 1.5$ (Table 12a)	$\approx +0.2$ $\rho_1 = 1.5$ (Table 12b)
Corner Radii, Table 13	+0.4	+0.4
Error Span	-5.0% to +7.7%	-0.1% to +5.6%

Assumed the most conservative case, $x' = 0$.

ACKNOWLEDGMENT

The author wishes to acknowledge the financial support and encouragement extended by Dr. R. Chait, Chief, Engineering Standardization Division of the Mechanics Engineering Laboratory; the aid given by D. M. Neal and D. Mason on the statistical aspects of brittle failure; and finally the constructively critical review, with patience, by W. W. Matthews.

REFERENCES

1. VAN REUTH, E. C. *The Advanced Research Projects Agency's Gas Turbine Program*. Proc. of the Second Army Materials Technology Conference - Ceramics for High Performance Applications, J. J. Burke, A. E. Gorum, and R. N. Katz, ed., Brook Hill Publishing Company, Chestnut Hill, Massachusetts, 1974.
2. TIMOSHENKO, S., and GOODIER, J. N. *Theory of Elasticity*. 2nd Ed., McGraw-Hill Book Co., Inc., New York, 1951.
3. CHAMLI, C. C. *Analysis of Three-Point-Bend Test for Materials with Unequal Tension and Compressive Properties*. NASA TN D7572, March 1974.
4. LEKHNITSKII, S. G. *Theory of Elasticity of an Anisotropic Elastic Body*. Holden-Day Series in Mathematical Physics, J. L. Brandstatter, ed., 1963, p. 204.
5. TIMOSHENKO, S. *Strength of Materials*. Parts I and II, D. Van Nostrand Co., Inc., New Jersey, 1976.
6. TIMOSHENKO, S. *Letter to the Editor*. Mechanical Engineering, v. 45, no. 4, April 1923, p. 259-260.
7. ASHWELL, D. G. *The Anticlastic Curvature of Rectangular Beams and Plates*. J. Roy., Aero. Soc., v. 54, 1950, p. 708-715.
8. WEST, D. C. *Flexure Testing of Plastics*. Exp. Mech., v. 21, no. 2, July 1964.
9. RITTER, J. E., and WILSON, W. R. D. *Friction Effects in Four-Point Bending*. ASLE Transactions, v. 18, no. 2, p. 130-134, presented at the 29th Annual Meeting, April 28-May 2, 1974.
10. TIMOSHENKO, S., and GERE, J. M. *Theory of Elastic Stability*. McGraw-Hill Book Co., Inc., New York, 1961.
11. RUDNICK, H., MARSCHALL, C. W., DUCKWORTH, W. H., and ENRICK, B. R. *The Evaluation and Interpretation of Mechanical Properties of Brittle Materials*. AFME TR 67-316, April 1968.
12. OH, H. L., and FINNIE, I. *On the Location of Fracture in Brittle Solids - I, Due to Static Loading*. Int. J. of Fracture Mechanics, v. 6, no. 3, September 1970, p. 287-300.
13. WEIBULL, W. *Statistical Theory of Strength of Materials*. Royal Swedish Institute for Engineering Res., Proc. no. 151, 1939, p. 1-45.
14. HOAGLAND, R. G., MARSCHALL, C. W., and DUCKWORTH, W. H. *Reduction of Errors in Ceramic Bend Tests*. J. Amer. Cer. Soc., v. 59, no. 5-6, May-June 1976, p. 189-192.
15. DUCKWORTH, W. H., et al. *Mechanical-Property Tests on Ceramic Bodies*. WADC TR 52-67, March 1952, p. 67-70.
16. NEWNHAM, R. C. *Strength Tests for Brittle Materials*. Proc. of the British Cer. Soc., no. 25, May 1975, p. 281-293.
17. WEIL, N. A. *Studies of Brittle Behaviour of Ceramic Materials*. ASD TR 61-628, Part II, April 1962, p. 38-42.
18. VON KARMAN, T., and SEEWALD, F. *Alhandl Aerodynam*. Inst. Tech. Hochschule, 1946, p. 256.
19. WESTWATER, J. W. *Flexure Testing of Plastic Materials*. Proc. ASTM, v. 49, 1949.
20. RICE, R. W. *Machining of Ceramics*. Proc. of the Second Army Materials Technology Conference - Ceramics for High Performance Applications, J. J. Burke, A. E. Gorum, and R. N. Katz, ed., Brook Hill Publishing Company, Chestnut Hill, Massachusetts, 1974.
21. RICE, R. W. *The Effect of Grinding Direction on the Strength of Ceramics*. The Science of Ceramics Machining and Surface Finishing, S. J. Scheider and R. W. Rice, ed., NBS Special Publication 348, Washington, DC, Government Printing Office (SD Catalog No. 13.10:348), 1972, p. 365-376.
22. DAVIS, D. G. S. *The Statistical Approach to Engineering Design in Ceramics*. Proc. Br. Ceramics Soc., no. 22, 1973, p. 429-452.
23. LEWIS, D., III. *An Experimental Test of Weibull Scaling Theory*. J. Amer. Cer. Soc., v. 59, no. 11-12, 1976, p. 507-510.
24. AMMRC Interim Report No.1 to MIL-HDBK 17, Composite Materials for Aircraft and Aerospace Applications (Proposed), December 1980.
25. DeSALVO, G. J. *Theory and Structural Design Applications of Weibull Statistics*. Westinghouse Astronuclear Laboratory, WANL-TME-2688, 1970.
26. McLEAN, A. F., and FISHER, E. A. *Brittle Materials Design, High Temperature Gas Turbine*. Ford Motor Company, Contract DAAG46-71-C-0162, Interim Report, AMMRC CTR 77-20, August 1977.
27. PALUSZNY, A., and WU, W. *Probabilistic Aspects of Designing with Ceramics*. Presented at the 22nd Annual Gas Turbine Conference of A.S.M.E., Philadelphia, Pa., March 27-31, 1977.
28. McLEAN, A. F., and BAKER, R. R. *Brittle Materials Design, High Temperature Gas Turbine*. Ford Motor Company, Contract DAAG46-71-C-0162, Interim Report, AMMRC CTR 76-31, October 1976.
29. THOMAN, D. R., BAIN, L. J., and ANTLE, C. E. *Inferences on the Parameters of Weibull Distribution*. Technometrics, v. 11, p. 445-460.

APPENDIX A. ANTICLASTIC CURVATURE

When a beam is bent by a moment, it produces a curvature ρ along its longitudinal axis; there is also curvature present in the transverse or lateral direction. This moment is defined by orthodox theory as

$$M_g = (EI/\rho)\beta \quad (A-1)$$

where β is a parameter representing anticlastic curvature after Ashwall.⁷

Since

$$\sigma_x = M_g c / I = (EI/\rho I) y \beta$$

then

$$\sigma_x = (Ey/\rho)\beta \quad (A-2)$$

where y is the distance from the neutral axis.

The β for such a beam of the simple case will equal 1.0 and if the beam width to depth is great, i.e., $b/d \rightarrow \infty$, the beam can be considered as a plate so that $\beta \rightarrow 1/(1-\nu^2)$. It is worthwhile to know the intermediate values of β such that the effect of anticlastic curvature on the error can be ascertained when assuming simple beam theory ($\beta = 1.0$) is valid.

Ashwall⁷ has determined β as a function of Poisson's ratio, beam width, depth, and neutral axis curvature by accounting for anticlastic curvature and treating the structure as a beam on an elastic foundation. The function β and related terms are repeated here in the following:

$$\beta = \frac{1}{1-\nu^2} + \frac{3}{2\gamma\beta} f(\gamma b) - \frac{2\sqrt{3}\nu}{\gamma b\sqrt{1-\nu^2}} F(\gamma b) \quad (A-3)$$

where

$$\gamma = \sqrt{\frac{4\sqrt{3(1-\nu^2)}}{d^2\rho^2}},$$

$$\begin{aligned} f(\gamma b) = & 2(B^2+C^2)[\sinh(\gamma b) + \sin(\gamma b)] \\ & + (B^2-C^2+2BC) \cosh(\gamma b) \sin(\gamma b) \\ & + (B^2-C^2-2BC) \sinh(\gamma b) \cos(\gamma b) \\ & + 2(B^2-C^2)(\gamma b), \end{aligned}$$

$$\begin{aligned} F(\gamma b) = & (B+C) \sinh(\gamma b/2) \cos(\gamma b/2) \\ & - (B-C) \cosh(\gamma b/2) \sin(\gamma b/2), \end{aligned}$$

*To be more exact, $b^2/\rho d \rightarrow \infty$.

$$B = \frac{\nu}{\sqrt{3(1-\nu^2)}} \left(\frac{\sinh(\gamma b/2) \cos(\gamma b/2) - \cosh(\gamma b/2) \sin(\gamma b/2)}{\sinh(\gamma b) + \sin(\gamma b)} \right), \text{ and}$$

$$C = \frac{\nu}{\sqrt{3(1-\nu^2)}} \left(\frac{\sinh(\gamma b/2) \cos(\gamma b/2) + \cosh(\gamma b/2) \sin(\gamma b/2)}{\sinh(\gamma b) + \sin(\gamma b)} \right).$$

The calculations performed for Table 4 in the text were accomplished in the following manner:

Since

$$\gamma b = b \sqrt{\frac{4(1-\nu^2)}{d^2 \rho^2}}, \text{ and } \rho = (E/\sigma)\nu\beta, \text{ then substituting into the above,}$$

allowing $y = d/2$, $E/\sigma = E/\sigma_b = 1 \times 10^3$, and $\nu = 0.25$ for ceramic materials, we have;

$$\gamma b \approx \frac{57.915 \times 10^{-3} (b/d)}{\sqrt{\beta}}. \quad (\text{A-4})$$

By programming (A-3) and *prescribing* b/d , but first allowing $\beta=1.0$, then iterating in the computer through (A-4), the relationship between b/d and β was obtained. Once this relationship is known, the percent error, defined as $[(1-\beta)/\beta]100$, as a function of b/d is realized. These errors are given in Table 4 as a function of b/d with $E/\sigma_b = 1 \times 10^3$ and $\nu = 0.25$.

APPENDIX B. LOAD MISLOCATION

Four-Point Loading

Consider the usual flexure testing setup where the loading head is rigidly attached to a testing machine, schematically shown in Figure 1b and idealized in Figure 1c. The upper loading head, where the inner span ℓ is fixed, can only translate in the vertical direction, and the lower support fixture, where the outer span L is fixed, can be located with reference to the loading head. The slope and deflection equations between points AB, BC, and CD are as follows:

$$\left. \begin{aligned} EI (dy_{AB}/dx) &= (P_1 x^2/2) + c_1 \\ EI y_{AB} &= (P_1 x^3/6) + c_1 x + c_2 \end{aligned} \right\} \quad (\text{B-1a})$$

$$\left. \begin{aligned} EI (dy_{BC}/dx) &= (P_1 - P_2)(x^2/2) + P_2 a_1 x + c_3 \\ EI y_{BC} &= (P_1 - P_2)(x^3/6) + (P_2 a_1 x^2/2) + c_3 x + c_4 \end{aligned} \right\} \quad (\text{B-1b})$$

and

$$\left. \begin{aligned} EI (dy_{CD}/dx) &= (P_1 - P_2 - P_3)(x^2/2) + P_2 a_1 x + P_3 (a_1 + \ell) x + c_5 \\ EI y_{CD} &= (P_1 - P_2 - P_3)(x^3/6) + (P_2 a_1 x^2/2) + P_3 (a_1 + \ell)(x^2/2) + c_5 x + c_6 \end{aligned} \right\} \quad (\text{B-1c})$$

where P_1 , P_2 , P_3 , and P_4 are the loads, x and y are defined as shown in Figure 1, E is the Young's modulus of the material, and I is the moment of inertia of the cross section of the beam.

Through the use of the various boundary conditions the constants are determined to be:

$$C_1 = -1/6 \{P_1(L^2 - a^2) + (P_2/L) [(a_1 - L)^3 + (\ell + a_2)a_2^2]\}$$

$$C_2 = 0$$

$$C_3 = -1/6 \{P_1(L^2 - a_2^2) + (P_2/L) [3a_1^2L - (a_2 + \ell)^3 + (\ell + a_2)a_2^2]\}$$

$$C_4 = P_2a_1^3/6$$

$$C_5 = -1/6 \{P_1L^2 + (P_2/L) [a_1^3 + 3a_1L^2 - L^3] + (P_3/L) [(a_1 + \ell)^3 + 3(a_1 + \ell)L^2 - L^3]\}$$

$$C_6 = P_3[(a_1 + \ell)^3/6] + (P_2a_1^3/6).$$

In order to determine the distribution of loading between the vertical loads P_1 , P_2 , P_3 , and P_4 , the final condition of equal deflection must be enforced at locations B and C (see Figure 1b), which is

$$(y_{BC})_{x=a_1} = (y_{BC})_{x=a_1+\ell}.$$

Enforcing the above condition in the second part of Equation B-1b results in

$$P_1/P_2 = -(\ell/L)^2 \left\{ \frac{\ell/L - (1 - a_1/L)(2 - \ell/L - 2a_1/L)}{(a_1/L)^3 - (a_1/L + \ell/L)^3 + \{1 - [1 - (\ell/L) - a_1/L]^2\}(\ell/L)} \right\}. \quad (B-2)$$

Utilizing force and moment equilibrium, a further relationship between all four forces is obtained and given in the following:

$$P_4/P_3 = \frac{(P_1/P_2)(a_1/L) + (P_1/P_2 - 1)\ell/L}{(P_1/P_2) - 1 + a_1/L} \quad \text{and} \quad P_3/P_2 = \frac{P_1/P_2 + a_1/L - 1}{1 - a_1/L - \ell/L}. \quad (B-3)$$

The ratio of the stress at x (σ_x) to the bending stress (σ_b) from Reference 14 or Equation 9 in the text, where it is assumed that $a_1 \neq a_2$, is:

$$\sigma_x/\sigma_b = \left[\frac{P_1}{\frac{P_2 + P_3}{2}} \right] \frac{x_1}{a} \quad (B-4)$$

where a is the value at a_1 with perfect load location and x_1 is defined as shown in Figure 1c.

By manipulation of (B-2) and (B-3), the factor $P_1/(P_2 + P_3)$ in (B-4) can be put into terms of a_1/L and ℓ/L . This was accomplished and the results are shown in the following equation:

$$\sigma_x/\sigma_b = \frac{[(a_1/L)/(a/L)](1 - a_1/L - \ell/L)[(\ell/L)(2 - a_1/L) - 2(1 - a_1/L)^2]}{3(a_1/L)(1 - \ell/L - a_1/L) - (1 - \ell/L)^2} \quad (B-5)$$

By defining the eccentricity of loading as $e/L = a_1/L - a/L$, Equation B-5 becomes:

$$\sigma_x/\sigma_b = \frac{[(e/L + a/L)/(a/L)][1 - (e/L + a/L) - \ell/L]\{(\ell/L)[2 - (e/L + a/L)] - 2[1 - (e/L + a/L)]^2\}}{3(e/L + a/L)[1 - \ell/L - (e/L + a/L)] - (1 - \ell/L)^2} \quad (B-6)$$

Calculations of σ_x/σ_b were obtained for the reference standard beams, where $\ell/L = 1/3$ as well as $\ell/L = 1/2$, by allowing e/L to take on negative values only in Equation B-6. Only negative values were considered because beam failure will occur due to a realistically larger moment than idealized when ignoring eccentricity. These error calculations although determined by allowing $e/L < 0$ in Equation B-6, are indicated as $\pm e/L$ in Table 6 for $\ell/L = 1/3$ and Table 7 for $\ell/L = 1/2$. This simply indicates that the location of the maximum moment or stress is at $x_1 = a_1$ when $e/L < 0$ and at $x_1 = a_1 + \ell$ when $e/L > 0$.

The reader is cautioned that for each value of ℓ/L there exists a set of limits on (B-2), (B-3), and (B-5). That is, a_1 can be such that either P_2 or P_3 can equal zero, because $(Y_{BC})_{x=a_1} \neq (Y_{BC})_{x=a_1+\ell}$ and the system changes from four-point to an eccentric three-point loading. The limiting values can be determined by allowing $P_2 = 0$ in Equation B-2. This was accomplished in terms of the load eccentricity ratio e/L for the reference standard beams, when $\ell/L = 1/3$, and found to be -0.0443 , and when $\ell/L = 1/2$, the result was -0.0465 . Thus Tables 6 and 7 do not extend beyond e/L of -0.0443 and -0.0465 .

APPENDIX C. BEAM TWISTING

If line loads are nonuniform or nonparallel between pairs of load contacts, or if the cross section of the specimen is skewed along its length, as shown in Figure 3, a net torque will result. The addition of torque gives rise to a maximum principal stress due to bending and torsional stresses.^{11,14} Failure assumed to be caused only by bending stress will yield an error. Two cases are considered: Case I - Failure occurs prior to specimen realignment in the bend fixture (bottoming), and Case II - Failure occurs at or after bottoming.

Case I

Recalling that the bending stress for a loaded beam is

$$\sigma_x = \sigma_b = 6M_b/bd^2 \quad (C-1)$$

where M_b is the measured bending moment at failure; for a four-point loaded beam $M_b = Pa$, and for a three-point loaded beam $M_b = PL/4$.

The shear stress due to torsion is²

$$\tau = T_b/k_2bd^2 \quad (C-2)$$

where T_b is the torque and equal to $P_b b$ for four-point bending and $P_b b/2$ for three-point bending, and k_2 is a numerical factor obtained from Reference 2 and is given in Table 9.

Prior to bottoming, the normal stress is

$$\sigma_n = (\sigma_z/2)(1-\cos 2\theta) + (\sigma_x/2)(1+\cos 2\theta) + \tau \sin 2\theta, \quad (C-3)$$

where θ is the angle of a plane inclined to the x axis. Since we shall assume a plane strain condition, i.e., $\epsilon_z = 0$, then

$$\epsilon_z = 0 = (1/E)(\sigma_z - \nu\sigma_x) \text{ or } \sigma_z = \nu\sigma_x = \nu\sigma_b$$

$$\sigma_n = (\sigma_b/2)[(1+\nu) + (1-\nu)\cos 2\theta] + \tau \sin 2\theta. \quad (C-4)$$

Now σ_n is maximum when

$$\tan 2\theta^* = 2\tau/(\sigma_x - \sigma_z);$$

but since

$$\sigma_z = \nu\sigma_x$$

then

$$\tan 2\theta^* = 2\tau/(1-\nu)\sigma_b. \quad (C-5)$$

where θ^* is the angle of a plane inclined to the axis at which principal stress is a maximum. Substitution of (C-1) and (C-2) into (C-5) for the condition prior to bottoming gives:

$$\tan 2\theta^* = (T_b/M_b)/[3(1-\nu)k_2], \quad (C-6)$$

$$\sin 2\theta^* = (T_b/M_b)/[(T_b/M_b)^2 + (3k_2)^2(1-\nu)^2]^{1/2}, \quad (C-7)$$

and

$$\cos 2\theta^* = [3k_2(1-\nu)]/[(T_b/M_b)^2 + (3k_2)^2(1-\nu)^2]^{1/2}. \quad (C-8)$$

Noting that

$$\tau = (\sigma_b/2)[(T_b/M_b)/3k_2], \quad (C-9)$$

and by substitution of the above relationships into (C-4) with some algebraic manipulation, we obtain:

$$\sigma_{n_{\max}} = (\sigma_b/2) \left\{ (1+\nu) + (1/3k_2)[(T_b/M_b)^2 + 9(1-\nu)^2k_2^2]^{1/2} \right\} \quad (C-10)$$

prior to bottoming. The shear stress due to torsion can be related to the twist angle² of the beam through the following relationship:

$$\tau = (k_1/k_2)Gd[(\phi_s/L_T) + (\phi_F/l')] \quad (C-11)$$

where ϕ_s is the twist angle along the length of the specimen, ϕ_F is the twist angle between a pair of load and contact points relative to ϕ_s , l' is equal to either "a" for four-point beam systems or $L/2$ for three-point beam systems, k_1 is another numerical factor² given in Table 9 and $G = E/2(1+\nu)$, the shear modulus of the material.

Equation (C-2) can be equated to (C-11) and thus we obtain:

$$T_{be} = [k_1 E / 2(1+\nu)] b d^2 [(d/L_T) \phi_s + (d/\ell') \phi_F] \quad (C-12)$$

where T_{be} is the torque when bottoming occurs. Thus, in order for (C-10) to be applicable, T_{be} must be equal to or greater than the torque provided by the bending moment, i.e., $T_b = (\ell'/b) M_b$ or $T_{be}/T_b \geq 1$, and from (C-2) and (C-12):

$$\begin{aligned} T_{be}/T_b &= [3k_1 E / \sigma_b (1+\nu) (b/\ell')] b d^2 [(d/L_T) \phi_s + (d/\ell') \phi_F] \geq 1.0, \text{ or} \\ n &= (b/\ell') [3k_1 (E/\sigma_b) / (1+\nu)] [(d/L_T) \phi_s + (d/\ell') \phi_F] \geq 1.0 \end{aligned} \quad (C-13)$$

where σ_b is the bending stress at failure according to (C-1).

Note that $T_b/M_b = b/\ell'$ and for four-point loading $\ell' = a$; for three-point loading $\ell' = L/2$, thus (C-10) becomes:

$$\sigma_{n_{\max}} = (\sigma_b/2) \left\{ (1+\nu) + (1/3k_2) [(1/(\ell'/b))^2 + 9(1-\nu)^2 k_2^2]^{1/2} \right\} \quad (C-14)$$

with $n = 1.0$.

Case II

If, however, $n < 1.0$ then bottoming occurs prior to or at failure and the following analysis is applicable:

Equations (C-4) and (C-5) are still appropriate but the shear stress is

$$\tau = T_{be} / k_2 b d^2. \quad (C-15)$$

Substitution of τ from the above and σ_b from (C-1) into (C-5) gives

$$\tan 2\theta^* = (T_{be}/M_b) / 3(1-\nu)k_2,$$

but from (C-13) $T_{be} = nT_b$ and thus:

$$\tan 2\theta^* = (nT_b/M_b) / 3(1-\nu)k_2. \quad (C-16)$$

As in Case I, using a like procedure we determine $\sigma_{n_{\max}}$ to be:

$$\sigma_{n_{\max}} = (\sigma_b/2) \left\{ (1+\nu) + (1/3k_2) [n^2 (T_b/M_b)^2 + 9(1-\nu)^2 k_2^2]^{1/2} \right\} \quad (C-17)$$

with

$$n = [3k_1 (E/\sigma_b) / (1+\nu)] [(d/L_T) \phi_s + (d/\ell') \phi_F] \leq 1.0. \quad (C-18)$$

Equation (C-17) is applicable to both systems since $(T_b/M_b) = b/\ell' = b/a$ for the three-point beam bending system, and $(T_b/M_b) = \ell'/b = 2b/L$ for the four-point system. Thus (C-17) becomes

$$\sigma_{n_{\max}} = (\sigma_b/2) \left\{ (1+\nu) + (1/3k_2) [(nb/\ell')^2 + 9(1-\nu)^2 k_2^2]^{1/2} \right\}. \quad (C-19)$$

Notice when $n = 1$, (C-19) reduces to (C-14).

Finally, the percent error is defined as:

$$\bar{\epsilon} = [(\sigma_b - \sigma_{n_{\max}}) / \sigma_{n_{\max}}] 100. \quad (C-20)$$

Errors were calculated in accordance with (C-20), with $\nu = 0.25$ for Case I ($n = 0.20, 0.40, 0.60$, and 0.80) and Case II ($n = 1.0$). These results are given in tabular form as a function of b/d and ℓ'/b in Tables 10a to 10e in the text.

APPENDIX D. WEDGING STRESSES

We allow the stress in the x direction in Figures 1 and 2 to be

$$\sigma_x = \sigma_b + (2P/bd)\beta_T, \quad (D-1)$$

where σ_b is the bending stress, i.e., $\sigma_b = (6M_x/bd^2)$, and $2P/bd$ is the local stress, i.e., the so-called wedging stress, and β_T is a numerical factor dependent on the normalized distance $x'/(d/2)$ on either side of the applied load point.²

For convenience the value of β_T at the tensile side of the beam as a function of $x'/(d/2)$ is given in Table D-1.

The percent error is defined as:

$$\bar{\epsilon} = [(\sigma_b - \sigma_x) / \sigma_x] 100, \quad (D-2)$$

and substitution of (D-1) into the above equation gives

$$\bar{\epsilon} = \left\{ -\beta_T / [(\sigma_b/2P/bd) + \beta_T] \right\} 100. \quad (D-3)$$

Since $\sigma_b = 6M_x/bd^2$, then (D-3) becomes:

$$\bar{\epsilon} = \left\{ -\beta_T / (3M_x/Pd + \beta_T) \right\} 100. \quad (D-4)$$

For a four-point loaded beam the bending moment is constant, i.e., $M_x = Pa$, and thus equation (D-4) becomes:

$$\bar{\epsilon} = \left\{ -\beta_T / [(3a/d) + \beta_T] \right\} 100. \quad (D-5)$$

From Table D-1 and Equation D-5 above, it is seen that the error is dependent on β_T or the fracture location, which is the normalized distance $x'/(d/2)$. These errors have been computed for the four-point loaded beam and presented in Table 11a.

For the three-point loaded beam, (D-4) is still applicable, but recalling that $M_x = P/2[(L/2) - x']$ and substituting M_x into (D-4) gives:

$$\bar{\epsilon} = \left\{ -\beta_T / \left(\frac{3}{4}(L/d) - \frac{3}{2}(x'/d) + \beta_T \right) \right\} 100. \quad (D-6)$$

Again, as can be seen by (D-6), the percent error is dependent upon β_T and the normalized fracture location. These percent errors are given in Table 11b.

Table D-1. WEDGING PARAMETER β_T

$\pm x'/d$	β_T
0	-0.1332
0.125	+0.0137
0.250	+0.0868
0.375	+0.0640
0.500	+0.0421
0.750	+0.0220
1.000	+0.0095
1.500	+0.00075

APPENDIX E. CONTACT POINT TANGENCY SHIFT

Consider the four-point loaded beam shown in Figure 4. The original span "a" is seen to decrease by the amount (h_1+h_2) due to rolling or slipping of the beam on its support and load points. The beam fulfills the condition:*

$$dy^2/dx^2 = M_X/EI. \quad (E-1)$$

The moments are defined as:

$$M_X = P(x-h_1), \quad 0 \leq x \leq (a-h_2)$$

$$M_X = P[a-(h_1+h_2)], \quad (a-h_2) \leq x \leq L-(a-h_2).$$

The slope equations are

$$EI(dy/dx) = P[(x^2/2)-h_1x] + C_1, \quad 0 \leq x \leq (a-h_2), \text{ and} \quad (E-2)$$

$$EI(dy/dx) = P[a-(h_1+h_2)]x + C_2, \quad (a-h_2) \leq x \leq L-(a-h_2). \quad (E-3)$$

Now when $x = a-h_2$,

$$C_1 + P \left\{ [(a-h_2)^2/2] - (a-h_2)h_1 \right\} = P[a-(h_1+h_2)](a-h_2) + C_2, \text{ or}$$

$$C_2 - C_1 = -(P/2)(a-h_2)^2. \quad (E-4)$$

Note also that when $x = L/2$ and $dy/dx = 0$ in (E-3),

$$C_2 = -P[a-(h_1+h_2)]L/2. \quad (E-5)$$

After substitution of C_2 into (E-4) we obtain:

$$C_1 = (P/2) \left\{ (a-h_2)^2 - L[a-(h_1+h_2)] \right\}. \quad (E-6)$$

*It is realized that a change in span dimensions must give rise to horizontal reactions; but it is assumed that this effect is small, and is thus ignored.

Substitution of these constants into the appropriate slope equations gives:

$$EI(dy/dx) = P[(x^2/2) - h_1x] + (P/2) \left\{ (a-h_2)^2 - L[a-(h_1+h_2)] \right\} \quad (E-7)$$

with $0 \leq x \leq (a-h_2)$, and

$$EI(dy/dx) = P[a-(h_1+h_2)][x-(L/2)], \quad (E-8)$$

with $(a-h_2) \leq x \leq L-(a-h_2)$.

Now when $x = h_1$ from the geometry $dy/dx = -h_1/\sqrt{R_1^2-h_1^2} \approx -h_1/R_1$ and when $x = a-h_2$, $dy/dx = -h_2/\sqrt{R_2^2-h_2^2} \approx -h_2/R_2$. The above relationships are used with (E-7) and (E-8) and we obtain:

$$(R_1/d) = \frac{(h_1/a)(E/\sigma_b)}{(h_1/a)^2 - (1-h_2/a)^2 + (L/a)[1-(h_1/a + h_2/a)]} \quad (E-9)$$

and

$$1-(h_2/a) = (1/2) \left\{ [(L/2a) + (h_1/a) + A_2] - \sqrt{[(L/2a) + (h_1/a) + A_2]^2 - 4[(h_1/a)(L/2a) + A_2]} \right\} \quad (E-10)$$

where $A_2 = (E/2\sigma_b)/(R_2/d)$.

Note that for the three-point loading case $h_2 = 0$, $L/a = 2$, and $P \rightarrow P/2$ and (E-9) reduces to:

$$R_1/d = [2(h_1/L)(E/\sigma_b)]/[(2h_1/L)-1]^2, \quad (E-11)$$

and the region of validity of (E-10) vanishes.

The percent error is defined as:

$$\bar{\epsilon} = [(\sigma_b - \sigma_x)/\sigma_x]100 = [(M_b - M_x)/M_x]100, \text{ or} \\ \bar{\epsilon} = \left\{ [(h_1/a) + (h_2/a)]/[1 - (h_1/a) - (h_2/a)] \right\} 100 \quad (E-12)$$

for four-point loading and

$$\bar{\epsilon} = \left\{ (2h_1/L)/[1 - (2h_1/L)] \right\} 100 \quad (E-13)$$

for three-point loading.

Calculations were performed by the following procedure. It was assumed that $E/\sigma_b = 1 \times 10^3$, and thus $A_2 = (1 \times 10^3)/(\rho_2/d)$; then for the 1/3- and 1/4-four-point loading case $a/L = 1/3$ and $1/4$, numerical values were assigned to ρ_2/d and h_1/a and then h_2/a was determined from (E-10). Those numerical values of h_1/a and corresponding h_2/a were substituted into (E-9) to determine ρ_1/d . This same procedure was used for the three-point loading case with $h_2 = 0$ and $L/a = 2$. Once the parameters h_1/a , h_2/a , ρ_2/d and ρ_1/d are known, percent errors according to (E-12)

for the four-point loading case and (E-13) for the three-point loading case can be determined. Such errors are given in Tables 12a-c.

APPENDIX F. ERROR DUE TO NEGLECTING CHANGE IN MOMENT OF INERTIA CAUSED BY CORNER RADII OR CHAMFERS

Corner Radius

Consider Figure 5a, which shows the cross section of a rectangular beam with corner radii r . The true moment of inertia $(I_{xx})_r$ about the centroidal or neutral axis $x-x$ is:

$$(I_{xx})_r = b(d-2r)^3/12 + (b-2r)r^3/6 + (1/2)(b-2r)(d-r)^2r + 2r^4(\pi/9 - 8/9\pi) + \pi r^2[d/2 - r(1 - 4/3\pi)]^2. \quad (F-1)$$

Most investigators, however, will neglect the loss of inertia when calculating the bending stress due to corner radii and assume that $I_b = bd^3/12$, and if we define the percent error as $\{[I_b - (I_{xx})_r]/(I_{xx})_r\}100$, we then obtain:

$$\bar{\epsilon} = \frac{1 - \left\{ (1-2r/d)^3 + 2[1-2(r/d)(d/b)](r/d)^3 + 6[1-2(r/d)(d/b)](1-r/d)^2(r/d) + 24(d/b)(r/d)^4(\pi/9-8/9\pi) + 12\pi(d/b)(r/d)^2[1/2-(r/d)(1-4/3\pi)]^2 \right\}}{(1-2r/d)^3 + 2[1-2(r/d)(d/b)](r/d)^3 + 6[1-2(r/d)(d/b)](1-r/d)^2(r/d) + 24(d/b)(r/d)^4(\pi/9-8/9\pi) + 12\pi(d/b)(r/d)^2[1/2-r/d(1-4/3\pi)]^2}. \quad (F-2)$$

45° Chamfer

Now consider Figure 5b, which shows a rectangular beam with 45° corner chamfers c . The true moment of Inertia $(I_{xx})_c$ about the $x-x$ axis is:

$$(I_{xx})_c = (bd^3/12) - (c^2/9)[c^2 + (1/2)(3d-2c)^2]. \quad (F-3)$$

Defining the error in the same manner as above results in:

$$\bar{\epsilon} = \left\{ \frac{(4/3)(d/b)(c/d)^2[(c/d)^2 + (1/2)(3-2c/d)^2]}{1 - (4/3)(d/b)(c/d)^2[(c/d)^2 + (1/2)(3-2c/d)^2]} \right\} 100. \quad (F-4)$$

The errors were calculated for various values of d/b as a function of r/d from (F-2) and c/d from (F-4). These results are shown in Tables 13 and 14.

DISTRIBUTION LIST

No. of Copies	To	No. of Copies	To
1	Office of the Under Secretary of Defense for Research and Engineering, The Pentagon, Washington, DC 20310	1	Commander, U.S. Army Tank-Automotive Research and Development Command, Warren, MI 48090
1	ATTN: Mr. J. Persh	1	ATTN: Dr. W. Bryzik
1	Dr. G. Gamota	1	Mr. E. Hamperian
12	Commander, Defense Technical Information Center, Cameron Station, Building 5, 5010 Duke Street, Alexandria, VA 22314	1	O. Rose
1	National Technical Information Service, 5285 Port Royal Road, Springfield, VA 22161	1	ORDTA-RKA, Dr. J. Chevalier
1	Director, Defense Advanced Research Projects Agency, 1400 Wilson Boulevard, Arlington, VA 22209	1	ORDTA-UL, Technical Library
1	ATTN: Dr. A. Bement	1	ORDTA-R
1	Dr. Van Reuth	1	Commander, U.S. Army Armament Research and Development Command, Dover, NJ 07801
1	MAJ Harry Winsor	1	ATTN: Mr. J. Lannon
1	Battelle Columbus Laboratories, Metals and Ceramics Information Center, 505 King Avenue, Columbus, OH 43201	1	Dr. G. Vezzoli
1	ATTN: Mr. Winston Duckworth	1	Mr. A. Graf
1	Dr. D. Niesz	1	Mr. Harry E. Peibly, Jr., PLASTEC, Director
1	Dr. R. Willis	1	Technical Library
1	Deputy Chief of Staff, Research, Development, and Acquisition, Headquarters, Department of the Army, Washington, DC 20310	1	Commander, U.S. Army Armament Materiel Readiness Command, Rock Island, IL 61299
1	ATTN: DAMA-ARZ	1	ATTN: Technical Library
1	DAMA-CSS, Dr. J. Bryant	1	Commander, Aberdeen Proving Ground, MD 21005
1	DAMA-PPP, Mr. R. Vawter	1	ATTN: DRDAR-CLB-PS, Mr. J. Vervier
1	Commander, U.S. Army Medical Research and Development Command, Fort Detrick, Frederick, MD 21701	1	Commander, U.S. Army Mobility Equipment Research and Development Command, Fort Belvoir, VA 22060
1	ATTN: SGRD-SI, Mr. Lawrence L. Ware, Jr.	1	ATTN: DRDME-EM, Mr. W. McGovern
1	Commander, Army Research Office, P.O. Box 12211, Research Triangle Park, NC 27709	1	DRDME-V, Mr. E. York
1	ATTN: Information Processing Office	1	DRDME-X, Mr. H. J. Peters
1	Dr. G. Mayer	1	Director, U.S. Army Ballistic Research Laboratory, Aberdeen Proving Ground, MD 21005
1	Dr. J. Hurt	1	ATTN: DRDAR-TSB-S (STINFO)
1	Commander, U.S. Army Materiel Development and Readiness Command, 5001 Eisenhower Avenue, Alexandria, VA 22333	1	Commander, Rock Island Arsenal, Rock Island, IL 61299
1	ATTN: DRCDMD-ST	1	ATTN: SARRI-EN
1	DRCLDC	1	Commander, U.S. Army Test and Evaluation Command, Aberdeen Proving Ground, MD 21005
1	Commander, U.S. Army Electronics Research and Development Command, Fort Monmouth, NJ 07703	1	ATTN: DRSTE-ME
1	ATTN: DELSD-L	1	Commander, U.S. Army Foreign Science and Technology Center, 220 7th Street, N.E., Charlottesville, VA 22901
1	Commander, U.S. Army Materiel Systems Analysis Activity, Aberdeen Proving Ground, MD 21005	1	ATTN: Military Tech, Mr. W. Marley
1	ATTN: DRXSY-MP, H. Cohen	1	Chief, Benet Weapons Laboratory, LCWSL, USA ARRADCOM, Watervliet, NY 12189
1	Commander, U.S. Army Night Vision Electro-Optics Laboratory, Fort Belvoir, VA 22060	1	ATTN: DRDAR-LCB-TL
1	ATTN: DELNV-S, Mr. P. Travesky	1	Commander, Watervliet Arsenal, Watervliet, NY 12189
1	DELNV-L-D, Dr. R. Buser	1	ATTN: Dr. T. Davidson
1	Commander, Harry Diamond Laboratories, 2800 Powder Mill Road, Adelphi, MD 20783	1	Director, Eustis Directorate, U.S. Army Mobility Research and Development Laboratory, Fort Eustis, VA 23604
1	ATTN: Mr. A. Benderly	1	ATTN: Mr. J. Robinson, DAVDL-E-MOS (AVRADCOM)
1	Technical Information Office	1	Mr. C. Walker
1	DELHD-RAE	1	Commander, U.S. Army Engineer Waterways Experiment Station, Vicksburg, MS 39180
1	Commander, U.S. Army Missile Command, Redstone Arsenal, AL 35809	1	ATTN: Research Center Library
1	ATTN: Mr. P. Ormsby	1	U.S. Army Munitions Production Base Modernization Agency, Dover, NJ 07801
1	Technical Library	1	ATTN: SARPM-PBM-P
1	DRSMI-TB, Redstone Scientific Information Center	1	Technical Director, Human Engineering Laboratories, Aberdeen Proving Ground, MD 21005
1	Commander, U.S. Army Aviation Research and Development Command, 4300 Goodfellow Boulevard, St. Louis, MO 63120	1	ATTN: Technical Reports Office
1	ATTN: DRDAV-EGX	1	Chief of Naval Research, Arlington, VA 22217
1	DRDAV-QE	1	ATTN: Code 471
1	Technical Library	1	Dr. A. Diness
1	Commander, U.S. Army Natick Research and Development Laboratories, Natick, MA 01760	1	Dr. R. Pohanka
1	ATTN: Technical Library	1	Naval Research Laboratory, Washington, DC 20375
1	Dr. J. Hanson	1	ATTN: Dr. J. M. Krafft - Code 5R30
1	Commander, U.S. Army Satellite Communications Agency, Fort Monmouth, NJ 07703	1	Mr. R. Rice
1	ATTN: Technical Document Center	1	Dr. Jim C. I. Chang
		1	Headquarters, Naval Air Systems Command, Washington, DC 20360
		1	ATTN: Code 5203
		1	Code MAT-042M

No. of Copies	To
1	Headquarters, Naval Sea Systems Command, 1941 Jefferson Davis Highway, Arlington, VA 22376 ATTN: Code 035
1	Headquarters, Naval Electronics Systems Command, Washington, DC 20360 ATTN: Code 504
1	Commander, Naval Ordnance Station, Louisville, KY 40214 ATTN: Code 25
1	Commander, Naval Material Industrial Resources Office, Building 537-2, Philadelphia Naval Base, Philadelphia, PA 19112 ATTN: Technical Director
1	Commander, Naval Weapons Center, China Lake, CA 93555 ATTN: Mr. F. Markarian 1 Mr. E. Teppo 1 Mr. M. Ritchie
1	Commander, U.S. Air Force of Scientific Research, Building 410, Bolling Air Force Base, Washington, DC 20332 ATTN: MAJ W. Simmons
1	Commander, U.S. Air Force Wright Aeronautics Laboratory, Wright-Patterson Air Dr. M. Lindley Force Base, OH 45433 ATTN: AFWAL/MLLM, Dr. N. Tallan 1 AFWAL/MLLM, Dr. H. Graham 1 AFWAL/MLLM, Dr. R. Ruh 1 AFWAL/MLLM, Dr. A. Katz 1 AFWAL/MLLM, Mr. K. S. Mazdiyasni 1 Aero Propulsion Labs, Mr. R. Marsh
1	Commander, Air Force Weapons Laboratory, Kirtland Air Force Base, Albuquerque, NM 87115 ATTN: Dr. R. Rudder
1	Commander, Air Force Armament Center, Eglin Air Force Base, FL 32542 ATTN: Technical Library
1	National Aeronautics and Space Administration, Washington, DC 20546 ATTN: Mr. G. C. Deutsch - Code RW 1 Mr. J. Gangler 1 AFSS-AD, Office of Scientific and Technical Information
1	National Aeronautics and Space Administration, Lewis Research Center, 21000 Brookpark Road, Cleveland, OH 44135 ATTN: J. Accurio, USAMRDL 1 Dr. H. B. Probst, MS 49-1 1 Dr. R. Ashbrook 1 Dr. S. Dutta 1 Mr. S. Grisaffe
1	National Aeronautics and Space Administration, Langley Research Center, Center, Hampton, VA 23665 ATTN: Mr. J. Buckley, Mail Stop 387
1	Commander, White Sands Missile Range, Electronic Warfare Laboratory, OMEW, ERADCOM, White Sands, NM 88002 ATTN: Mr. Thomas Redder, DRSEL-WEM-ME
1	Department of Energy, Division of Transportation, 20 Massachusetts Avenue, N.W., Washington, DC 20545 ATTN: Mr. George Thur (TEC) 1 Mr. Robert Schulz (TEC) 1 Mr. John Neal (CLNRT) 1 Mr. Steve Wander (Fossil Fuels)
1	Department of Transportation, 400 Seventh Street, S.W., Washington, DC 20590 ATTN: Mr. M. Lauriente
1	Mechanical Properties Data Center, Belfour Stulen Inc., 13917 W. Bay Shore Drive, Traverse City, MI 49684
1	National Bureau of Standards, Washington, DC 20234 ATTN: Dr. S. Wiederhorn 1 Dr. J. B. Wachtman
1	National Research Council, National Materials Advisory Board, 2101 Constitution Avenue, Washington, DC 20418 ATTN: D. Groves 1 R. M. Springs

No. of Copies	To
1	National Science Foundation, Washington, DC 20550 ATTN: B. A. Wilcox
1	Admiralty Materials Technology Establishment, Polle, Dorset BH16 6JU, UK ATTN: Dr. D. Godfrey 1 Dr. M. Lindley
1	AiResearch Manufacturing Company, AiResearch Casting Company, 2525 West 190th Street, Torrance, CA 90505 ATTN: Mr. K. Styhr 1 Dr. D. Kotchick
1	AiResearch Manufacturing Company, Materials Engineering Dept., 111 South 34th Street, P.O. Box 5217, Phoenix, AZ 85010 ATTN: Mr. D. W. Richerson, MS 93-393/503-44 1 Dr. W. Carruthers
1	AVCO Corporation, Applied Technology Division, Lowell Industrial Park, Lowell, MA 01887 ATTN: Dr. T. Vasilos
1	Carborundum Company, Research and Development Division, P.O. Box 1054, Niagara Falls, NY 14302 ATTN: Dr. J. A. Coppola
1	Case Western Reserve University, Department of Metallurgy, Cleveland, OH 44106 ATTN: Prof. A. H. Heuer
1	Ceradyne, Inc., P.O. Box 11030, 3030 South Red Hill Avenue, Santa Ana, CA 92705 ATTN: Dr. Richard Palicka
1	Combustion Engineering, Inc., 911 West Main Street, Chattanooga, TN 37402 ATTN: C. H. Sump
1	Cummins Engine Company, Columbus, IN 47201 ATTN: Mr. R. Kamo
1	Defence Research Establishment Pacific, FMO, Victoria, B.C., VOS 1B0, Canada ATTN: R. D. Barer
1	Deposits and Composites, Inc., 1821 Michael Faraday Drive, Reston, VA 22090 ATTN: Mr. R. E. Engdahl
1	Electric Power Research Institute, P.O. Box 10412, 3412 Hillview Avenue, Palo Alto, CA 94304 ATTN: Dr. A. Cohn
1	European Research Office, 223 Old Marylebone Road, London, NW1 - 5the, England ATTN: Dr. R. Quattrone 1 LT COL James Kennedy
1	FMC Corporation, 1105 Coleman Avenue, Box 1201, San Jose, CA 95108 ATTN: Dr. A. E. Gorum, Manager of Advanced Technology Ordnance Engineering Division
1	Ford Motor Company, Turbine Research Department, 20000 Rotunda Drive, Dearborn, MI 48121 ATTN: Mr. A. F. McLean 1 Mr. E. A. Fisher 1 Mr. J. A. Mangels 1 Mr. R. Govila
1	General Atomic Company, P.O. Box 81608, San Diego, CA 92138 ATTN: Jim Halzgraf
1	General Electric Company, Mail Drop H-99, Cincinnati, OH 45215 ATTN: Mr. Warren Nelson
1	General Electric Company, Research and Development Center, Box H, Schenectady, NY 12345 ATTN: Dr. R. J. Charles 1 Dr. C. D. Greshovich 1 Dr. S. Prochazka
1	General Motors Corporation, AC Spark Plug Division, Flint, MI 48156 ATTN: Dr. M. Berg

No. of Copies	To
1	Georgia Institute of Technology, EES, Atlanta, GA 30332 ATTN: Mr. J. D. Walton
1	GTE Laboratories, Waltham Research Center, 40 Sylvan Road, Waltham, MA 02154
1	ATTN: Dr. C. Quackenbush
1	Dr. W. H. Rhodes
1	IIT Research Institute, 10 West 35th Street, Chicago, IL 60616
1	ATTN: Mr. S. Bortz, Director, Ceramics Research
1	Dr. D. Larsen
1	Institut fur Werkstoff-Forschung, DFVLR, 505 Porz-Wahn, Linder Hohe, Germany
1	ATTN: Dr. W. Bunk
1	Institut fur Werkstoff-Forschung, DFVLR, 5000 Koln 90(Porz), Linder Hohe, Germany
1	ATTN: Dr. Ing Jurgen Heinrich
1	International Harvester, Solar Division, 2200 Pacific Highway, P.O. Box 90966, San Diego, CA 92138
1	ATTN: Dr. A. Metcalfe
1	Ms. M. E. Gulden
1	Jet Propulsion Laboratory, C.I.T., 4800 Oak Grove Drive, Pasadena, CA 91103
1	ATTN: Dr. Richard Smoak
1	Kawecki Berylco Industries, Inc., P.O. Box 1462, Reading, PA 19603
1	ATTN: Mr. R. J. Longenecker
1	Mr. Edward Kraft, Product Development Manager, Industrial Sales Division, Kyocera International, Inc., 8611 Balboa Avenue, San Diego, CA 92123
1	Martin Marietta Laboratories, 1450 South Rolling Road, Baltimore, MD 21227
1	ATTN: Dr. J. Venables
1	Massachusetts Institute of Technology, Department of Metallurgy and Materials Science, Cambridge, MA 02139
1	ATTN: Prof. R. L. Coble
1	Prof. H. K. Bowen
1	Prof. W. D. Kingery
1	Prof. R. Cannon
1	Materials Research Laboratories, P.O. Box 50, Ascot Vale, VIC 3032, Australia
1	ATTN: Dr. C. W. Weaver
1	Midwest Research Institute, 425 Volker Boulevard, Kansas City, MO 64110
1	ATTN: Mr. Gordon W. Gross, Head, Physics Station
1	Dr. Howard Mizuhara, GTE-Wesgo, 477 Harbor Boulevard, Belmont, CA 94002
1	Norton Company, Worcester, MA 01606
1	ATTN: Dr. N. Ault
1	Dr. M. L. Torti
1	Pennsylvania State University, Materials Research Laboratory, Materials Science Department, University Park, PA 16802
1	ATTN: Prof. R. Roy
1	Prof. R. E. Newnham
1	Prof. R. E. Tressler
1	Prof. R. Bradt
1	Prof. V. S. Stubican
1	Pratt and Whitney Aircraft, P.O. Box 2691, West Palm Beach, FL 33402
1	ATTN: Mr. Mel Mendelson
1	PSC, Box 1044, APD San Francisco 96328
1	ATTN: MAJ A. Anthony Borges
1	RIAS, Division of the Martin Company, Baltimore, MD 21203
1	ATTN: Dr. A. R. C. Westwood
1	Rockwell International Science Center, 1349 Camino Dos Rios, Thousand Oaks, CA 91360
1	ATTN: Dr. F. Lange

No. of Copies	To
1	Royal Aircraft Establishment, Materials Department, R 178 Building, Farnborough, Hants, England
1	ATTN: Dr. N. Corney
1	Shane Associates, Inc., 7821 Carleigh Parkway, Springfield, VA 22152
1	ATTN: Dr. Robert S. Shane, Consultant
1	Silag Inc., P.O. Drawer H, Old Buncombe at Poplar Greer, SC 29651
1	ATTN: Dr. Bryant C. Bechtold
1	Solar Turbine International, 2200 Pacific Coast Highway, San Diego, CA 92138
1	ATTN: Mr. Andrew Russel, Mail Zone R-1
1	Stanford Research International, 333 Ravenswood Avenue, Menlo Park, CA 94025
1	ATTN: Dr. P. Jorgensen
1	Dr. D. Rowcliffe
1	State University of New York at Stony Brook, Department of Materials Science, Long Island, NY 11790
1	ATTN: Prof. Franklin F. Y. Wang
1	TRW Defense and Space Systems Group, Redondo Beach, CA 90278
1	ATTN: Francis E. Fendell
1	United Technologies Research Center, East Hartford, CT 06108
1	ATTN: Dr. J. Brennan
1	Dr. F. Galasso
1	University of California, Department of Materials Science and Engineering, Hearst Building, Berkeley, CA 94720
1	ATTN: Dr. D. Clarke
1	University of California, Lawrence Livermore Laboratory, P.O. Box 808, Livermore, CA 94550
1	ATTN: Mr. R. Landingham
1	Dr. C. F. Cline
1	University of Florida, Department of Materials Science and Engineering, Gainesville, FL 32601
1	ATTN: Dr. L. Hench
1	University of Massachusetts, Department of Mechanical Engineering, Amherst, MA 01003
1	ATTN: Prof. K. Jakus
1	Prof. J. Ritter
1	University of Newcastle Upon Tyne, Department of Metallurgy and Engineering Materials, Newcastle Upon Tyne, NE1 7 RU, England
1	ATTN: Prof. K. H. Jack
1	University of Washington, Ceramic Engineering Division, FB-10, Seattle, WA 98195
1	ATTN: Prof. James I. Mueller
1	Virginia Polytechnic Institute, Department of Materials Engineering, Blacksburg, VA 24061
1	Prof. D. P. H. Hasselman
1	Westinghouse Electric Corporation, Research Laboratories, Pittsburgh, PA 15235
1	ATTN: Dr. R. J. Bratton
1	Dr. B. Rossing
1	Mr. Joseph T. Bailey, 3M Company, Technical Ceramic Products Division, 3M Center, Building 207-1W, St. Paul, MN 55101
1	Dr. Jacob Stiglich, Dart Industries/San Fernando Laboratories, 10258 Morris Avenue, Pacoima, CA 91331
1	Dr. J. Petrovic - CMB-5, Mail Stop 230, Los Alamos Scientific Laboratories, Los Alamos, NM 87545
1	Mr. R. J. Zentner, EAI Corporation, 198 Thomas Johnson Drive, Suite 16, Frederick, MD 21701
2	Director, Army Materials and Mechanics Research Center, Watertown, MA 02172
2	ATTN: DRXMR-PL
2	Author

Army Materials and Mechanics Research Center,
Watertown, Massachusetts 02172
REQUIREMENTS FOR FLEXURE TESTING
OF BRITTLE MATERIALS -
Francis I. Baratta

AD

UNCLASSIFIED
UNLIMITED DISTRIBUTION

Key Words

Mechanical tests
Flexural strength
Brittle materials

Technical Report AMRC TR 82-20, April 1982, 46 pp -
illus-tables, AMCMS Code 728012.13

Requirements for accurate bend-testing of four-point and three-point beams of rectangular cross-section are outlined. The so-called simple beam theory assumptions are examined to yield beam geometry ratios that will result in minimum error when utilizing elasticity theory. Factors that give rise to additional errors when determining bend strength are examined, such as: wedging stress, contact stress, load mislocation, beam twisting, friction at beam contact points, contact point tangency shift, and neglect of corner radii or chamfer in the stress determination. Also included are the appropriate Weibull strength relationships and an estimate of errors in the determination of the Weibull parameters based on sample size. Error tables, based on many of the previously mentioned factors, are presented.

Such data are utilized to rationally arrive at a 1/3-four-point and a three-point beam of a specific geometry ratio and dimension that will result in minimization of errors during flexure testing. Although such beams are recommended for a military standard, they are termed reference standard beams. Beams of other loading configurations and dimensions are considered acceptable if statistical correlation to one of the reference standards is determined, and if error spans are reported when presenting flexure test data.

Army Materials and Mechanics Research Center,
Watertown, Massachusetts 02172
REQUIREMENTS FOR FLEXURE TESTING
OF BRITTLE MATERIALS -
Francis I. Baratta

AD

UNCLASSIFIED
UNLIMITED DISTRIBUTION

Key Words

Mechanical tests
Flexural strength
Brittle materials

Technical Report AMRC TR 82-20, April 1982, 46 pp -
illus-tables, AMCMS Code 728012.13

Requirements for accurate bend-testing of four-point and three-point beams of rectangular cross-section are outlined. The so-called simple beam theory assumptions are examined to yield beam geometry ratios that will result in minimum error when utilizing elasticity theory. Factors that give rise to additional errors when determining bend strength are examined, such as: wedging stress, contact stress, load mislocation, beam twisting, friction at beam contact points, contact point tangency shift, and neglect of corner radii or chamfer in the stress determination. Also included are the appropriate Weibull strength relationships and an estimate of errors in the determination of the Weibull parameters based on sample size. Error tables, based on many of the previously mentioned factors, are presented.

Such data are utilized to rationally arrive at a 1/3-four-point and a three-point beam of a specific geometry ratio and dimension that will result in minimization of errors during flexure testing. Although such beams are recommended for a military standard, they are termed reference standard beams. Beams of other loading configurations and dimensions are considered acceptable if statistical correlation to one of the reference standards is determined, and if error spans are reported when presenting flexure test data.

Army Materials and Mechanics Research Center,
Watertown, Massachusetts 02172
REQUIREMENTS FOR FLEXURE TESTING
OF BRITTLE MATERIALS -
Francis I. Baratta

AD

UNCLASSIFIED
UNLIMITED DISTRIBUTION

Key Words

Mechanical tests
Flexural strength
Brittle materials

Technical Report AMRC TR 82-20, April 1982, 46 pp -
illus-tables, AMCMS Code 728012.13

Requirements for accurate bend-testing of four-point and three-point beams of rectangular cross-section are outlined. The so-called simple beam theory assumptions are examined to yield beam geometry ratios that will result in minimum error when utilizing elasticity theory. Factors that give rise to additional errors when determining bend strength are examined, such as: wedging stress, contact stress, load mislocation, beam twisting, friction at beam contact points, contact point tangency shift, and neglect of corner radii or chamfer in the stress determination. Also included are the appropriate Weibull strength relationships and an estimate of errors in the determination of the Weibull parameters based on sample size. Error tables, based on many of the previously mentioned factors, are presented.

Such data are utilized to rationally arrive at a 1/3-four-point and a three-point beam of a specific geometry ratio and dimension that will result in minimization of errors during flexure testing. Although such beams are recommended for a military standard, they are termed reference standard beams. Beams of other loading configurations and dimensions are considered acceptable if statistical correlation to one of the reference standards is determined, and if error spans are reported when presenting flexure test data.

Army Materials and Mechanics Research Center,
Watertown, Massachusetts 02172
REQUIREMENTS FOR FLEXURE TESTING
OF BRITTLE MATERIALS -
Francis I. Baratta

AD

UNCLASSIFIED
UNLIMITED DISTRIBUTION

Key Words

Mechanical tests
Flexural strength
Brittle materials

Technical Report AMRC TR 82-20, April 1982, 46 pp -
illus-tables, AMCMS Code 728012.13

Requirements for accurate bend-testing of four-point and three-point beams of rectangular cross-section are outlined. The so-called simple beam theory assumptions are examined to yield beam geometry ratios that will result in minimum error when utilizing elasticity theory. Factors that give rise to additional errors when determining bend strength are examined, such as: wedging stress, contact stress, load mislocation, beam twisting, friction at beam contact points, contact point tangency shift, and neglect of corner radii or chamfer in the stress determination. Also included are the appropriate Weibull strength relationships and an estimate of errors in the determination of the Weibull parameters based on sample size. Error tables, based on many of the previously mentioned factors, are presented.

Such data are utilized to rationally arrive at a 1/3-four-point and a three-point beam of a specific geometry ratio and dimension that will result in minimization of errors during flexure testing. Although such beams are recommended for a military standard, they are termed reference standard beams. Beams of other loading configurations and dimensions are considered acceptable if statistical correlation to one of the reference standards is determined, and if error spans are reported when presenting flexure test data.

Army Materials and Mechanics Research Center,
Watertown, Massachusetts 02172
REQUIREMENTS FOR FLEXURE TESTING
OF BRITTLE MATERIALS -
Francis I. Baratta

AD

UNCLASSIFIED
UNLIMITED DISTRIBUTION

Key Words

Technical Report AMRC TR 82-20, April 1982, 46 pp -
illus-tables, AMCS Code 728012.13

Mechanical tests
Flexural strength
Brittle materials

Requirements for accurate bend-testing of four-point and three-point beams of rectangular cross-section are outlined. The so-called simple beam theory assumptions are examined to yield beam geometry ratios that will result in minimum error when utilizing elasticity theory. Factors that give rise to additional errors when determining bend strength are examined, such as: wedging stress, contact stress, load mislocation, beam twisting, friction at beam contact points, contact point tangency shift, and neglect of corner radii or chamfer in the stress determination. Also included are the appropriate Weibull strength relationships and an estimate of errors in the determination of the Weibull parameters based on sample size. Error tables, based on many of the previously mentioned factors, are presented.

Such data are utilized to rationally arrive at a 1/3-four-point and a three-point beam of a specific geometry ratio and dimension that will result in minimization of errors during flexure testing. Although such beams are recommended for a military standard, they are termed reference standard beams. Beams of other loading configurations and dimensions are considered acceptable if statistical correlation to one of the reference standards is determined, and if error spans are reported when presenting flexure test data.

Army Materials and Mechanics Research Center,
Watertown, Massachusetts 02172
REQUIREMENTS FOR FLEXURE TESTING
OF BRITTLE MATERIALS -
Francis I. Baratta

AD

UNCLASSIFIED
UNLIMITED DISTRIBUTION

Key Words

Technical Report AMRC TR 82-20, April 1982, 46 pp -
illus-tables, AMCS Code 728012.13

Mechanical tests
Flexural strength
Brittle materials

Requirements for accurate bend-testing of four-point and three-point beams of rectangular cross-section are outlined. The so-called simple beam theory assumptions are examined to yield beam geometry ratios that will result in minimum error when utilizing elasticity theory. Factors that give rise to additional errors when determining bend strength are examined, such as: wedging stress, contact stress, load mislocation, beam twisting, friction at beam contact points, contact point tangency shift, and neglect of corner radii or chamfer in the stress determination. Also included are the appropriate Weibull strength relationships and an estimate of errors in the determination of the Weibull parameters based on sample size. Error tables, based on many of the previously mentioned factors, are presented.

Such data are utilized to rationally arrive at a 1/3-four-point and a three-point beam of a specific geometry ratio and dimension that will result in minimization of errors during flexure testing. Although such beams are recommended for a military standard, they are termed reference standard beams. Beams of other loading configurations and dimensions are considered acceptable if statistical correlation to one of the reference standards is determined, and if error spans are reported when presenting flexure test data.

Army Materials and Mechanics Research Center,
Watertown, Massachusetts 02172
REQUIREMENTS FOR FLEXURE TESTING
OF BRITTLE MATERIALS -
Francis I. Baratta

AD

UNCLASSIFIED
UNLIMITED DISTRIBUTION

Key Words

Technical Report AMRC TR 82-20, April 1982, 46 pp -
illus-tables, AMCS Code 728012.13

Mechanical tests
Flexural strength
Brittle materials

Requirements for accurate bend-testing of four-point and three-point beams of rectangular cross-section are outlined. The so-called simple beam theory assumptions are examined to yield beam geometry ratios that will result in minimum error when utilizing elasticity theory. Factors that give rise to additional errors when determining bend strength are examined, such as: wedging stress, contact stress, load mislocation, beam twisting, friction at beam contact points, contact point tangency shift, and neglect of corner radii or chamfer in the stress determination. Also included are the appropriate Weibull strength relationships and an estimate of errors in the determination of the Weibull parameters based on sample size. Error tables, based on many of the previously mentioned factors, are presented.

Such data are utilized to rationally arrive at a 1/3-four-point and a three-point beam of a specific geometry ratio and dimension that will result in minimization of errors during flexure testing. Although such beams are recommended for a military standard, they are termed reference standard beams. Beams of other loading configurations and dimensions are considered acceptable if statistical correlation to one of the reference standards is determined, and if error spans are reported when presenting flexure test data.

Army Materials and Mechanics Research Center,
Watertown, Massachusetts 02172
REQUIREMENTS FOR FLEXURE TESTING
OF BRITTLE MATERIALS -
Francis I. Baratta

AD

UNCLASSIFIED
UNLIMITED DISTRIBUTION

Key Words

Technical Report AMRC TR 82-20, April 1982, 46 pp -
illus-tables, AMCS Code 728012.13

Mechanical tests
Flexural strength
Brittle materials

Requirements for accurate bend-testing of four-point and three-point beams of rectangular cross-section are outlined. The so-called simple beam theory assumptions are examined to yield beam geometry ratios that will result in minimum error when utilizing elasticity theory. Factors that give rise to additional errors when determining bend strength are examined, such as: wedging stress, contact stress, load mislocation, beam twisting, friction at beam contact points, contact point tangency shift, and neglect of corner radii or chamfer in the stress determination. Also included are the appropriate Weibull strength relationships and an estimate of errors in the determination of the Weibull parameters based on sample size. Error tables, based on many of the previously mentioned factors, are presented.

Such data are utilized to rationally arrive at a 1/3-four-point and a three-point beam of a specific geometry ratio and dimension that will result in minimization of errors during flexure testing. Although such beams are recommended for a military standard, they are termed reference standard beams. Beams of other loading configurations and dimensions are considered acceptable if statistical correlation to one of the reference standards is determined, and if error spans are reported when presenting flexure test data.